
Article:
Aslam, Z, Li, H orcid.org/0000-0002-2670-874X, Hammerton, J et al. (1 more author) (2022) Combustion and Emissions Performance of Simulated Syngas/Diesel Dual Fuels in a CI Engine. SAE Technical Papers. 2022-01-1051. ISSN 0148-7191

https://doi.org/10.4271/2022-01-1051

2022-01-1051

Combustion and emissions performance of simulated syngas/diesel dual fuels in a CI engine

Author, co-author (Do NOT enter this information. It will be pulled from participant tab in MyTechZone)

Affiliation (Do NOT enter this information. It will be pulled from participant tab in MyTechZone)

Abstract

Small diesel engines are a common primer for micro and mini-grid systems, which can supply affordable electricity to rural and remote areas, especially in developing countries. These diesel generators have no exhaust after-treatment system thus exhaust emissions are high. This paper investigates the potential of introducing simulated synthetic gas (syngas) to diesel in a small diesel engine to explore the opportunities of widening fuel choices and reducing emissions using a 5.7kW single cylinder direct injection diesel generator engine. Three different simulated syngas blends (with varying hydrogen content) were prepared to represent the typical syngas compositions produced from downdraft gasification and were injected into the air inlet. In-cylinder pressure, ignition delay, premixed combustion, combustion stability, specific energy consumption (SEC), and gaseous and particle emissions were measured at various power settings and mixing ratios. Particle size distributions (PSD) were measured by DMS500, and gaseous emissions were measured by the HORIBA MEXA7100 series. The correlations between combustion and emission performance and mixing ratios and substitution ratios were investigated. Dual fuel operation led to a decrease in diesel consumption, thermal efficiency, NO_x, and NO emissions and an increase in THC and CO emissions. For all dual fuel tests, a reduction in the total particle number concentration (TPNC) was noted while the particle size distribution curves remained unchanged relative to diesel baseline data at all engine loads except for 30%. At 30% engine load, the change in the particle size distribution curves was dependent on the syngas blend used. The syngas with the highest hydrogen content showed superior combustion performance relative to the other syngas blends evaluated due to shorter ignition delay times and higher maximum in-cylinder pressure values, thus producing lower THC and CO emissions, but higher NO_x emissions.

Introduction

Diesel generators (often referred to as diesel gensets) are commonly used for the generation of electricity. The use of diesel gensets is more commonplace in rural and remote areas, especially in developing countries that have no access to the national grid [1]. Often the genset is not always the cheapest choice for producing electricity. For example, in Tanzania, the high cost of diesel fuel results in such off-grid systems having a substantially higher running cost (per kWh) than the grid [2-4]. Hence in countries such as these, the high cost and dependency on fossil fuels when running off-grid diesel generators are impediments to sustainable and economic development [3, 5]. Therefore, the use of renewable, sustainable, and affordable fuels is a key to producing more affordable green electricity in such areas [5, 6].

One of the approaches is to use the synthetic gas (syngas) derived from the gasification of biomass as a fuel in the diesel generators, i.e., syngas/diesel dual fuel engines. Syngas is produced by a thermal chemical process called gasification, in which biomass undergoes partial oxidation. The typical composition of such syngas contains hydrogen (H_2), carbon monoxide (CO), carbon dioxide (CO_2), nitrogen (N_2), and methane (CH_4), and in some cases trace amounts of oxygen too.

This paper looks at utilising syngas in dual fuel mode within a diesel engine where diesel is used as the pilot fuel. The type of syngas most suitable for use within diesel engines is that generated from the downdraft gasification process due to its lower particulate matter (PM) and tar content [7, 8]. Developing countries that have a plentiful supply of waste biomass residues [5, 9, 10] can utilise waste biomass residues as a feedstock for gasification thus enabling the production of more sustainable electricity as well as increasing access to electricity. The diesel engine can be adapted to run in syngas-diesel mode by using Reactivity Controlled Compression Ignition (RCCI, at the high syngas substitution ratios) where two different fuels with differing reactivities are required [6, 11, 12].

Dual fuel studies using simulated binary syngas (only containing H_2 and CO)

Various dual fuel studies have been conducted using simulated syngas which contains only H_2 and CO as they represent the main fuel component of syngas. Sahoo et al. [13] conducted research into syngas-diesel dual fueling using a single-cylinder, 5.2 kW, 1,500 RPM engine using such simulated syngas. The engine performance was monitored at various loads between 20 to 100%. Lower brake thermal efficiency (BTE) values were reported for dual fuel mode versus pure diesel due to the poorer combustion performance of the syngas (especially at lower loads) compared to diesel. Lower NO_x emissions and in-cylinder peak pressures were obtained in dual fuel mode, the reduction in peak pressure was due to the slower heat release and a longer ignition delay. Engine exhaust gas temperatures, CO, and hydrocarbons (HC) emissions all increased in dual fuel mode. The CO increase was attributed to the CO content in the syngas. A maximum diesel substitution of ~59% was calculated at 80% engine load in dual fuel mode. The paper concluded that the benefits of syngas-diesel mode are the NO_x reduction, and the negatives (the increase in HC and CO emissions) could be overcome by increasing the H_2 content or the H_2/CO ratio of the syngas.

Their next study involved studying the effects of varying the H_2/CO content of the syngas using the same equipment [14]. Three fuel blends were examined in dual fuel mode: 100% hydrogen, syngas 1 containing 75:25 H_2/CO, and another having a 50:50 H_2/CO volume ratio. Higher brake thermal efficiency values were reported with the increase in the H_2 content of the syngas at high loads. The brake thermal efficiency values decreased for all dual fuel modes as previously seen [13]. The highest in-cylinder pressures and combustion temperatures were reported for 100% H_2 resulting in higher NO_x emissions and exhaust gas temperatures in comparison to the other gaseous fuels tested. The CO emissions increased when using syngas with a higher CO content in dual fuel mode. It was concluded that higher hydrogen content results in lower CO and HC emissions due to the higher flame speed.

Bika et al. [15] also investigated the effects of differing amounts of hydrogen and CO content in simulated syngas using a single-cylinder engine at 1,825 RPM speed. Testing was carried out at two power conditions: 2 and 4 bar net indicated mean effective pressure ($IMEP_n$) using diesel substitution values of 10, 20, and 40% of the syngas in dual fuel mode. This research showed that the brake thermal efficiency decreased in dual fuel mode relative to diesel at both power conditions as seen by other researchers [13] due to incomplete combustion resulting in unburnt syngas passing into the exhaust. Bika et al. [15] also reported that at 2 bar $IMEP_n$, the NO_x levels were unaffected and remained constant for all test conditions. However, at 4 bar $IMEP_n$, the NO_x emissions increased with increasing syngas substitution. These NO_x results were contradictory to those reported by Sahoo et al. [13]. Additionally, the NO_2/NO_x ratio doubled with syngas substitution for all the test conditions evaluated, this was attributed to an increase in the amount of HO_2 radicals which react with the NO to form NO_2.

Mahmood et al. [16] also studied the combustion characteristics of syngas-diesel dual fuelling whereby numerical simulations were carried out on a single cylinder Ricardo-Hydra 2,000 RPM diesel engine. Simulated binary syngas (containing 50:50 H_2 and CO) was evaluated at various ratios ranging between 10 to 50% at a lambda value of 1.6. ANSYS workbench 16.1 software was used to calculate the effects of syngas addition. These simulation results showed that the brake thermal efficiency increased in dual fuel mode, also the peak in-cylinder temperature and pressure increased with the syngas fraction, which was higher than diesel baseline data. The CO, NO, and CO_2 emissions increased with increasing syngas fraction addition, with all dual fuel emissions being higher than diesel baseline values.

Dual fuel studies using a simulated multicomponent syngas

A research review was conducted below whereby researchers have used simulated syngas that mimics the typical composition of syngas produced from the gasification process. Guo et al. [17] studied the effects of three different simulated syngas blends which contained H_2, CO, N_2, and CO_2 in dual fuel mode in terms of engine performance and emissions (including soot). The composition of the syngas blends chosen represented the following: syngas 1: typically produced from a downdraft air blown gasifier, syngas 4: typically produced from oxygen blow downdraft gasifier, and syngas 5 represented syngas 1 but with a different H_2 to CO ratio. Guo et al. [17] used a modified single-cylinder version of a 75 kW engine single cylinder with a fixed speed of 910 RPM and brake mean specific pressure (BMEP) values of 4.05 and 8.10 bar. The syngas fractions evaluated were 0, 25, and 50 % at 4.05 bar and 0, 25, 50, and 60 % at 8.10 bar. The relative air/fuel ratio was fixed at 2.75 and 2.17, and the intake temperature was maintained at 40 °C. The findings from this study generally showed a slight drop in brake thermal efficiency at low and medium loads, which are in line with that reported by other researchers in this field [13, 15].

This study reported that in dual fuel mode, at low loads, the CO levels increased but at medium load conditions, the initial introduction of syngas lead the CO emissions to increase, but after this further syngas addition did not affect the CO emissions further. Syngas types with a higher H_2/CO ratio or a lower inert content produced lower soot emissions, hence the soot emissions were directly dependent on the syngas composition. Dual fuel mode also saw a reduction in NO_x emissions due to the lower cylinder temperatures and poorer combustion. This reduction in NO_x emissions agreed with the findings reported by some researchers [13], but not by others [15]. Additionally, it was also reported that the intake pressure saw a marginal increase with increasing syngas fraction at a fixed speed/load.

Kousheshi et al. [18] investigated dual fuelling using a 2.44 L, single cylinder RCCI engine via experimental numerical analysis to determine the effects of syngas on the engine exhaust emissions and performance. This study was based on the syngas-diesel RCCI engine maintaining constant energy per cycle. This study evaluated three different syngas types whose composition was based on that typically produced by gasification containing varying amounts of H_2, CO, CH_4, CO_2, N_2, and C_2H_4/C_2H_6. These gases varied from each other in terms of the H_2/CO ratio (% vol). These gases were also compared to simulated syngas which contained 50:50 H_2 to CO. The findings reported were that using simulated gasifier syngas led to higher soot, CO, and unburnt hydrocarbons (UHC) in comparison to the simulated binary syngas. Also, the peak pressure and maximum local temperatures increased significantly with an increasing ratio of H_2. With the increase in hydrogen, shorter ignition delay (ID), a sharper heat release rate (HRR), reduced soot, CO, and UHCs were reported alongside an increase in NO_x emissions.

Tuan and Luong [19] also conducted a numerical simulation study whereby they investigated the effects of dual fuelling using simulated syngas whose composition represented that produced by a small-scale downdraft gasifier fed by charcoal. The composition of the syngas (% vol) used was: 11.63 H_2, 24.47 CO, 0.01 CH_4, 0.08 O_2, 1.79 CO_2, and 62.02 N_2. Of the studies discussed here, this was the first to include trace amounts of oxygen in the composition of the syngas. This study was based on a 3-cylinder, 8.75 kW power diesel engine typically used in a small genset at an engine speed of 1,500 RPM. Various models were used to simulate the combustion characteristics, and heat transfer and to calculate emissions of NO_x, CO, and soot. This study showed that at full load conditions (at an indicated mean effective pressure of 6.54 bar), dual fuelling could reduce diesel consumption by 60%, similar to the value reported by Sahoo et al [13]. In dual fuel mode, the specific energy consumption (SEC), CO, and NO_x emissions increased, however, the soot emissions decreased as the amount of syngas used increased. This reported increase in NO_x emissions in this study is contradictory to other findings of similar studies discussed earlier [13, 17]. The increase in NO_x emissions was explained by an increase in the in-cylinder temperature which increased with increasing syngas fraction.

Olanrewaju et al. [6] investigated the effect of dual fuels on the heat release rate (HRR) behaviour and combustion phasing using an improved HRR model. The study was based on experimental work using a single cylinder, RCCI mode CI engine with a maximum power rating of 5.7 kW engine. The effects of syngas substitution (by energy) were studied at 10, 25, and 45% syngas substitution at 1 to 4-kW loads (generator output). The simulated syngas used had a composition that mimicked that produced from a typical downdraft gasifier which contained 15% H_2, 20% CO, 4% methane, 12% CO_2, 48.02% nitrogen, and 0.98% oxygen (% mol); the same engine lab and one of the syngas blends used in this study (SGA) were used by these researchers [6].

These authors reported that as the amount of syngas added increased, the HRR profile shifted to the right, away from the diesel baseline reference curve at each engine load tested. This was stated to be a direct effect of the reduction in the cetane number of the dual fuel mixture which increased with the addition of syngas, thus reducing its tendency to autoignite. This was further corroborated by their ignition delay (ID) data which showed that the ID increased with increasing syngas at all loads evaluated.

These authors [6] also reported that the start of combustion, peak pressure, and peak heat release rate all occurred later in syngas-diesel mode (in CAD) compared to diesel baseline, which agreed with other researchers [19, 20]. This was attributed to a longer injection delay in dual fuel mode [13, 17, 20], which increased with the increasing syngas fraction. Also, in dual fuel mode, a reduction in the peak pressure and peak temperature were noted relative to the diesel baseline. The decrease in peak temperature in this study was said to be related to a reduction in the flame temperature with increasing syngas fraction. In addition, the duration of combustion (DoC), all increased with increasing syngas addition at generator loads of 1 to 3kW. This was explained as a direct result of the slower and delayed combustion caused by the presence of the CO component in the syngas. At full load (4kW), the DoC did not see this increase, a slight decrease was noted with increasing syngas substitution. Hence, it can be said that the DoC in dual fuel combustion for syngas-diesel is load and flow rate dependent. The findings regarding the peak of heat release rate (PoHRR) were higher than the diesel baseline was observed at full and medium high engine loads, at the lowest syngas fraction (10% GEF). Similar findings were reported by Tuan and Luong [19] who also reported higher PoHRR in dual fuel combustion. This was attributed to the hydrogen content of the syngas having a faster flame speed, which promotes more homogeneous combustion. When looking at the effects of the hydrogen content of the syngas in dual fuel combustion, the literature reports that syngas blends containing higher hydrogen content had lower injection delays and higher peak pressure values than those with lower hydrogen content [18, 21]. Hence, a higher hydrogen content of syngas is said to promote fuller combustion.

In terms of particle emissions from syngas-diesel studies, various studies focus on the effect of the syngas dual fuelling on soot emissions whereby the syngas composition contains hydrogen and CO only [22, 23]. In general, it is reported that syngas-diesel dual fuelling reduces the particulate emissions when conveyed as a filter smoke number [22]. A combined experimental and computational study by Chuahy et al. [24] looked at the particle size distribution (PSD) in syngas-diesel using reformate i.e. syngas containing hydrogen and CO. The particle measurements were analysed using a scanning mobility particle sizer. This study showed that in dual fuel operation (using energy fractions as low as 25%), the PSD curves changed compared to pure diesel. In dual fuel mode, the particle concentration related to accumulation mode decreased while the nucleation mode particle concentration increased. These changes in the PSD were attributed to reductions in fuel stratification and not due to changes in the soot surface chemistry. A further experimental study (using syngas containing H_2 and CO) reported reductions in transient soot emissions measured using an AVL 439 opacimeter [23].

Overall, the literature reviewed indicates that the majority of studies have reported a reduction in PM mass, smoke density, and concentration in dual fuel mode using syngas-diesel relative to diesel baseline. Ramadhas et al. [25] reported a reduction in the smoke density in dual fuel mode when using real syngas directly from gasification relative to the diesel baseline. The smoke density increased with increasing syngas fraction. Other studies have looked at the PM mass (expressed as specific emissions in g/kWh) and have reported a reduction in PM mass in dual fuel mode relative to the diesel baseline [16, 19, 26-29].

The reductions in soot emissions, (expressed in g/kWh) decreased with increasing syngas addition [17, 19, 26, 28] and were all lower than the diesel baseline. There are limited studies that have looked at the change in the PSD when using gasifier-based syngas (real or simulated) in dual fuel mode. The findings from the study by Hernandez et al. [27] which used real syngas cannot be directly compared to the findings from this paper due to the differences in the engine speed and engine operational conditions.

Dual fuel studies using gasifiers directly coupled with diesel engines

Hernandez et al. [27] conducted a dual fuel study in 2014, using an AVL 501 single cylinder, 1,500 RPM, DI engine, equipped with EGR and a common rail injection system. The syngas used has a composition resembling that produced from steam gasification of dealcoholised marc of grapes. The particle number and size distribution were determined using a Scanning Mobility Particle Size (SMPS) which measured the particle diameter size up to 100 nm with and without the use of EGR. This study concluded that the dual fuel mode PM mass and concentration were lower than the diesel baseline data alongside a reduction in the particle mean diameter. Both the PM mass and concentration decreased with increasing syngas fraction. This reduction was thought to be due to a reduction in the use of diesel fuel (source of particulates), in addition to the higher concentration of OH radicals, derived from the hydrogen content in the syngas. The OH radicals are thought to promote soot oxidation. Also, the volatile organic fraction of the PM was reported to increase whilst the PM decreased in dual fuel mode, this was said to be possibly due to the extra adsorbed unburned CO and CH_4 on the porous soot. This is the only study reviewed that has looked at the particle number and particle size distribution (PSD) in syngas-diesel combustion using syngas which contains more than just CO and hydrogen.

Other relevant research in this field is that conducted by Uma et al. [29] and Rinaldi et al. [7] which involved the dual fuelling of a diesel engine with syngas which was produced and fed in from a connected gasification unit. Uma et al. [29] used real syngas produced from a downdraft gasifier whose typical feedstock was wood and briquettes made from forestry and crop waste residues. The syngas generated was cooled and cleaned before being fed into the diesel engine. The test engine used was a turbocharged, direct injection six cylinder, vertical, four stroke diesel engine with a speed of 1500 RPM and a power rating of 77.2kW, coupled with an alternator. The typical syngas composition used was 19% CO, 14% H_2, 1.9% CH_4, and 10% CO_2, with the balance being nitrogen. The syngas-diesel experiments were carried out at various loads from 10 to 40 kW. The findings from this study showed that the brake thermal efficiency value decreased as did the NO_x, SO_2, and PM emissions when in dual fuel mode relative to pure diesel. However, an increase in the CO and HC emissions was recorded in dual fuel mode compared to pure diesel.

Rinaldi et al.[7] used a constant speed (3,000 RPM), 4-stroke, 4-cylinder, 2.7 litre, turbocharged diesel test engine equipped with a 160 MPa Common Rail injection system and a high pressure EGR circuit. The syngas was produced using wood chips in an air blown downdraft gasifier and the syngas produced was cooled and cleaned before entering the engine. Three different loads were tested which were 16, 31, and 94 kW. The composition of the dry syngas produced was 9.4% H_2. 59.4% N_2, 22.4% CO, 5.4% CO_2, and 3.4% CH_4. This research showed that the maximum diesel substitution rate was limited by the production rate of the syngas from the gasifier, therefore higher powers were not reached. The maximum diesel substitution rate reached was 60% at a power of 16 kW, a similar value to that reported by other researchers discussed here [13, 19].

Technically, the limitations caused by the production rate of the syngas from the gasifier can be overcome by storing and compressing syngas for the application of small-scale generation [15]. This study reported an increase in the brake thermal efficiency in dual fuel mode, as did Mahmood et al [16], both these reported increases in brake thermal efficiency contradict all other findings reported [13, 15, 17, 29]. Also, this study showed that in-cylinder pressure traces for pure diesel and syngas-diesel were similar, again this is contradictory to previous research [13, 17]. This study concluded that the use of syngas in dual fuel is beneficial in reducing diesel consumption and improving combustion quality.

To summarise this discussion, contradictory results have been reported for brake thermal efficiency, in-cylinder peak pressure, and NO_x emissions when in dual fuel mode using syngas-diesel relative to pure diesel. Also, there is more agreement in the literature whereby the majority consensus states that the THC and CO emissions increase in syngas-diesel dual fuel mode. In terms of emissions, most researchers have looked at CO, HC, NO_x, and to a lesser extent PM. There is a need to further investigate the resulting exhaust emissions from syngas-diesel dual fuel in more detail by considering the NO, NO_2, and particulate emissions, especially in terms of PSD and total particle number concentration.

There is limited work conducted on a small high-speed diesel genset engine (3,000 RPM) which investigates the emissions produced using simulated 'gasifier' based syngas, i.e., that typically produced from a downdraft gasifier ran using waste biomass residues as feedstock. The work carried out by Olanrewaju et al. [6] used the same engine/lab setup and one of the simulated syngas blends: syngas A (SGA) tested in this work, but the focus of their study was the HRR and combustion phasing. Furthermore, there are limited studies that compare the effects of the variation in the hydrogen or H_2/CO ratios using simulated 'gasifier' based syngas. Of the studies which have, these have been conducted using slower speed engines ≤1,500 RPM [17, 18]. The effect of the hydrogen content is particularly important in controlling the resulting CO and HC emissions [14, 15, 18].

Hence there is no single comprehensive study that looks at the effect on the engine combustion performance together with the resulting emissions using simulated 'gasifier' syngas with a high-speed small engine. The need to have one single comprehensive study is important as it is difficult to compare data across studies as there are too many variables that affect the engine performance. Some examples include engine design, the operating parameters (such as speed, pilot fuel injection timing, pilot fuel mass, compression ratio, and inlet manifold conditions), as well as the gaseous fuel type [30]. Also, the basis of studies found in the literature varies as highlighted, some work is based solely on numerical analysis/simulations, thus comparison becomes tricky. Hence this paper provides a comprehensive study whereby the combustion performance and resulting emissions have been investigated using three different gasifier based simulated syngas with varying hydrogen content (and H_2/CO ratio). There are limited studies that have researched the impact of the hydrogen content of the syngas using gasifier-based syngas (real or simulated). Of key importance is that the simulated gasifier syngas chosen is that produced from a downdraft gasifier using waste biomass residues as its feedstock. Hence, this opens the potential of producing more affordable electricity whilst reducing the dependency on fossil fuels for those that rely on the use of diesel gensets for small-scale power generation.

Methodology

Experimental set up – test engine

An MG6000 SSY (MHM plant, UK) 6 kVA generator was used for this study. This incorporated a 5.7kW rated single-cylinder diesel engine which was adapted for dual fuels use (gas-diesel). The cylinder head on the genset engine was drilled and a thread tapped directly above the inlet port to allow the syngas 'injector' to inject as close to the inlet valve. The delivery of the gaseous fuel was controlled by an omega mass flow meter. The bottled gas was piped through stainless-steel pipework equipped with a two-stage regulator and a stainless-steel flashback arrester. The single-phase 50Hz generator (socket 230V,32A) was connected to the load bank. The engine specifications are shown in Table 1.

Table 1. Engine specifications

Parameter	**Specifications**
Manufacturer/Model	Yanmar LV Series, 2019 Model, L100V5
Emission compliance	EU Stage V emission complaint
Type	4-stroke, single cylinder, air cooled
Rated Power	5.7 kW
Speed	3,000 RPM
Bore x Stroke	86 mm x 75 mm
Compression Ratio	20.9:1
Total cylinder volume	457.55 cm^3
Fuel injector	FB injector, 5 holes, 0.185 mm hole diameter, 150° cone angle
Injection Pressure (diesel)	19.6 MPa
Engine oil capacity	1.7 L

Engine related instrumentation

The equipment and software used for data collection during the testing from the genset engine are summarised in Table 2. The in-cylinder pressure was measured using a pressure transducer connected to the Flexifem charge amplifier, this converted the charge into a voltage. This had a measuring range from 0 to 250 bar, with a sensitivity of 19 pico coulomb/bar. The RPM was calculated from the pressure data (360 pulses/rotation) by using the initial crankshaft point of rotation when the piston is at the top dead centre (at peak pressure), and by assuming a constant angular velocity. This provided the time interval for four strokes, hence the average interval between 10 of these events was used to calculate the RPM. The crank angle degree (CAD) was also determined using the pressure sensor and was detected when ~20 bar pressure was reached on the compression stroke. This is before combustion has begun and occurs at the same angle, i.e., when the TDC pressure equates to 0 CAD. The algorithm to calculate the RPM and CAD was previously written into the LabView software. The CAD had a resolution of 0.5 CAD. The engine itself was connected to a digital fuel balance which monitored diesel fuel usage in increments of 10g. The gaseous fuel was metered into the engine on a volume basis using an omega mass flow meter. The omega (FMA-2613A-V2) flow meter used had a reading accuracy of ±0.8% with the capacity of delivering 4 to 1000 standard litres per minute. Data from the engine, pressure sensor, thermocouples, fuel balance, and gas flow meter fed into the 8-slot Compact Rio chassis (National Instruments). Data logging and visualising were conducted using an in-house programme written into the LabView software.

Table 2. Engine related instrumentation

Parameter	Equipment specification
In-cylinder pressure	AVI FlexIFEM Indi 601, AVL GH14D transducer
Diesel fuel usage	Digital Scales- ADAM (CPW plus-35)
Syngas flow	Omega FMA-2613A-V2 Mass flow meter
Temperature	K-type thermocouples (x6)
Load output	Hillstone HAC2410-10. Single phase resistive load bank
Alternator	Linz E1C10M H

Emission measurements

The particle size distribution (PSD) was measured using the DMS500 MKII Fast Particle Analyser which is equipped with an integrated two-stage dilution system. The PSD was measured from 4.87 to 1,000 nm over 38 individual different sizes. Gaseous emissions were measured using the Horiba MEXA-7100D automobile emission analysers for NO_x, CO, CO_2, and THC. NOx was measured using Chemiluminescence.

Carbon dioxide (CO_2) and carbon monoxide (CO) were analysed using Non-Dispersive Infrared Spectroscopy (NDIR). The Total Hydrocarbons (THCs) were analysed using flame ionisation detection (FID) technique.

Fuel properties

Ultra-Low Sulfur Diesel fuel (ULSD/red diesel) was used for this study (BS 2869, 2010, Class A2 complaint). Elemental analysis was carried out on the fuel for Carbon (C), Hydrogen (H), and Nitrogen (N) content. The lower heating value (LHV) was determined using the bomb calorimeter (instrument PARR6200). The properties of the red diesel fuel are listed in Table 3. The density (ρ), LHV, and the stoichiometric air to flow ratio ($AFR_{stoich\text{-}gas}$) for each syngas were calculated whereby one mole of syngas was used as the basis. The composition and the calculated properties for each of the simulated syngas blends (purchased from BOC), labelled as syngas A, B, and C (SGA, SGB, and SGC), are summarised in Tables 4 and 5, respectively.

Table 3. Properties of red diesel

Property	Lab data	Specification data [31]
ρ @15 °C (kg/m^3)	0.84	0.820 minimum
LHV (MJ/kg)	44.19	N/A
Carbon (wt%)	85.90	87 (typical)
Hydrogen (wt%)	14.10	12.75 (typical)
Nitrogen (wt%)	~ 0	0.01-0.05 (typical)
Cetane Number (CN)	Not measured.	45 (minimum), 48 (typical)

Table 4. Composition of the simulated syngas blends

	Composition (mol %)					
Syngas:	**CH_4**	**H_2**	**CO**	**O_2**	**CO_2**	**N_2**
SGA	4	15	20	0.98	12	48.02
SGB	4	20	20	0.98	12	43.02
SGC	4	25	20	0.98	12	38.02

Table 5. Calculated properties of the simulated syngas blends

	Calculated values per syngas:		
Syngas	**LHV (MJ/kg)**	**ρ (kg/m^3)**	**$AFR_{stoich\ syngas}$**
SGA	4.886	1.067	1.316
SGB	5.645	1.013	1.527
SGC	6.491	0.959	1.763

Experimental procedure

Before conducting any tests, the engine was warmed up using red diesel fuel until the engine oil temperature reached a minimum of 50°C. Once warm, the required testing load was selected, and the engine was allowed to stabilise using diesel. Once stable, data logging was commenced for that load condition using diesel to obtain diesel baseline (DBL) data for ~10 minutes.

After diesel base logging, the syngas was added at the required flow rate and allowed to stabilise for 3-5 mins in dual fuel mode; any data generated during this period was discarded. Once stable in dual fuel mode, the clock time was recorded, and the engine ran in dual-fuel mode for a further 10 minutes at the selected gas flow rate, this data generated here forth was used for data analysis. Between every change in the gas flow rate or load, the engine was allowed to equilibrate for a minimum of 3-5 minutes in dual-fuel mode at the inputted gas flow. Again, this part of the data was not analysed from any instrument. The volume of gas added corresponded to a % syngas energy fraction (*% GEF*) in total fuel energy (diesel + syngas) which was calculated using Eq. (A1) in the Appendix. In terms of error bars, ± one standard deviation has been used which has been derived from repeat experimental work.

The experimental test conditions in terms of engine load and *% GEF* used at the corresponding generator output loads of 4, 3, 2, and 1 kW are summarised in Table 6. Experiments using high '*% GEF*' were only assessed at high loads due to a limited syngas supply.

Table 6. A summary of the experiments conducted and the test conditions

Generator load (kW)	**Load %max.**	***% GEF* evaluated**				
4.2 ±0.2	96 ±1.0	0	9.5 (±0.5)	22 (± 1.0)	38 (±1.5)	46 (±1.0)
3.3 ±0.2	76±4.0	0	9.5 (±0.5)	22 (± 1.0)	38 (±1.5)	
2.2±0.2	53.5 ±2	0	9.5 (±0.5)	22 (± 1.0)		
1.2±0.2	30 ±1	0	9.5 (±0.5)	22 (± 1.0)		

Data Analysis

The peak pressure was determined from the pressure crank angle degree (P-CAD) plots generated by averaging 100 cycles by the LabView software.

Start of Combustion (SoC) and Ignition Delay (*ID*)

The SoC was determined from the 1st and 2nd derivative plots of the P-CAD data. This was identified by the minimum of the 2nd derivative curve and the start point of the continuous rise in pressure from the first derivative [32]. The *ID* was calculated in crank angle degree (CAD) using Eq. (A2) in the Appendix. An illustrative graph is shown identifying the SoC using the methodology described using the P-CAD plots, this is shown in Figure 1.

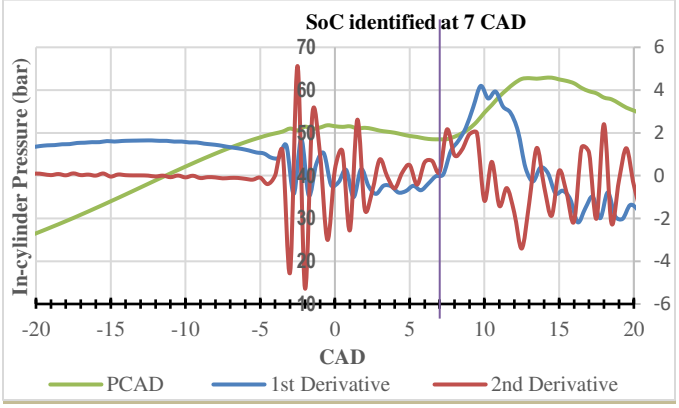

Figure 1. P-CAD plot generated during dual fuel combustion at full load which illustrates the identification of the SoC

Air to Fuel Ratio (AFR).

When running diesel baseline test conditions, standard diesel fuel parameters were inputted into the Mexa 7100D thus enabling the instrument to calculate the AFR value using the built-in software program based on the Brettschneider/Spindt equation [33]. As the mass of the air intake was not measured directly, the AFR for dual fuel runs (AFR_{df}) was calculated. First, the mass of the direct air was calculated using diesel baseline data at each condition using Eq. (1).

$$m_{DBL\,air} = (AFR_{DBL}\ x\ m_d) \quad (1)$$

$m_{DBL\,air}$ is the mass of air intake in pure diesel mode, kg/h

AFR_{DBL} is the air to fuel ratio as calculated by the MEXA instrument.

m_d is the mass flow rate of diesel used for diesel baseline, kg/h

Next, it was assumed that the addition of gaseous fuel would directly displace the air, thus reducing the mass of air in dual fuel mode. The mass of the air intake in dual fuel mode was calculated using Eq. (2).

$$m_{DF\,air} = \left(m_{DBL\,air} - m_g\right) \quad (2)$$

$m_{DF\,air}$ is the mass of air intake in dual fuel mode, kg/h

$m_{DBL\,air}$ is the mass of air intake in pure diesel mode, kg/h

m_g is the mass flow rate of syngas, kg/h

The dual-fuel Air to fuel Ratio (AFR_{df}) was calculated using Eq. (3). The dual-fuel mass was taken as the combined mass of both fuels.

$$AFR_{df} = \left(\frac{m_{DF\,air}}{m_{pd} + m_g}\right) \quad (3)$$

AFR_{df} is the air to fuel ratio by mass in dual fuel mode

$m_{DF\,air}$ is the mass of air intake in dual fuel mode, kg/h

m_g is the mass flow rate of syngas, kg/h

m_{pd} is the mass flow rate of pilot diesel in dual fuel mode, kg/h

The following parameters were also calculated from the data using the Equations summarised in the Appendix as follows:

Specific fuel consumption (*SFC*) for diesel baseline, Eq. (A3)
Specific energy consumption (SEC_{df}) for dual fuel mode Eq. (A4)
BTE for dual fuel mode was calculated using Eq. (A5)
BTE for diesel baseline was calculated using Eq. (A6)
The diesel replacement rate (*Z*) was calculated using Eq. (A7)
The Φ in dual fuel mode was calculated using Eq. (A8)
The Φ for DBL was calculated using Eq. (A9)

Emission index (*EI*)

Direct gaseous emissions were measured using the MEXA (in % or ppm). This average data was converted into emission index (*EI*) values [34] expressed as g/kg fuel using Eq. (A10) in the Appendix. The *EI* (g/kg fuel) was converted further and expressed as g/MJ fuel using Eq. (A11) in the Appendix. The data representing the LHV of the dual fuel was calculated using by Eq. (A12) as shown in the Appendix.

Specific emissions (SE)

The *Gas EI* data was converted to specific emissions (*SE*) in g/kWh [29] using Eq. (A13) in the Appendix.

Results and discussions

This section is split into three categories: engine combustion performance, gaseous emissions, and particulate emissions.

Engine combustion performance

Brake Thermal Efficiency (*BTE*), and Specific Energy Consumption (*SEC*)

For all the syngas fuels tested, as the % *GEF* increased, the brake thermal efficiency decreased, an example of the typical trend is shown in Figure 2 for SGB-diesel. This was expected as seen by most of the researchers when using syngas/dual fuel blends [13, 15, 17, 29, 30]. The reduction seen here in *BTE* values in dual-fuel mode could be explained by the poorer combustion performance, which is more apparent at lower loads [13, 14]. Also, lower *BTE* values in dual-fuel mode seen here could be linked to slower burning rates and lower P_{max} (peak in-cylinder pressures) [13]. Interestingly, the two studies reviewed and discussed earlier that reported an increase in *BTE* in dual fuel mode did not see a corresponding decrease in the in-cylinder pressure [7, 16]. This reduction in *BTE* observed for all syngas/diesel blends corresponded to an increase in specific energy consumption values for all syngas blends tested. The increase in specific energy consumption data with increasing % *GEF* is illustrated in Figure 3 using SGB-diesel as an example.

The specific energy consumption results in Figure 3 enable a convenient way for the comparisons of fuel/energy consumption between different studies and engines.

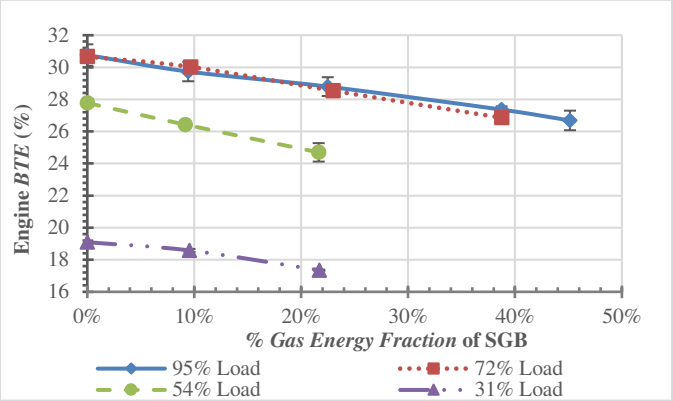

Figure 2. *Brake thermal efficiency (BTE)* data with increasing syngas fraction across all engine loads for SGB-diesel

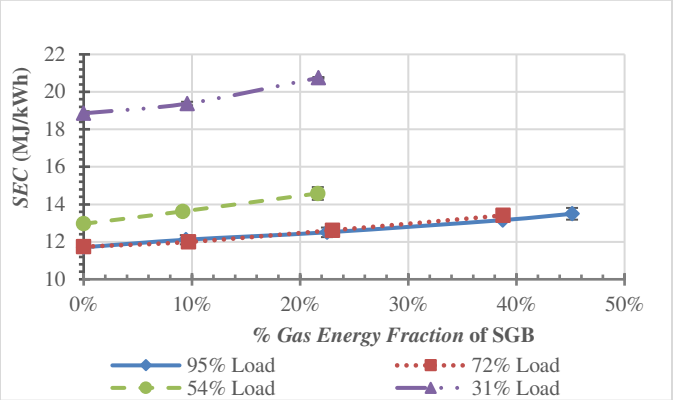

Figure 3. S*pecific Energy Consumption (SEC)* data with increasing syngas fraction across all engine loads for SGB-diesel

Overall, the brake thermal efficiency of syngas-diesel dual fuel is considered to be lower due to the high CO content present in the syngas [13] and this is seen from the analysis of the gaseous emissions. It is widely accepted that to improve the brake thermal efficiency of such dual-fuel blends, an increase in the hydrogen fraction is beneficial.

In addition, improving the H_2/CO ratio, especially in the lean mixture condition is recommended [13, 35]. The fractions of H_2 and CO significantly affect combustion due to their different combustion characteristics. CO can affect the reactivity of a syngas mixture; oxidation of CO with H_2 present is known to affect the syngas oxidation mechanism [36]. Also, the CO in the syngas becomes trapped in crevices in the combustion chamber, away from the flame, thereby remaining unburnt and present in the exhaust gases [18]. Thus, increasing the H_2 content of the syngas should result in a higher in-cylinder pressure as H_2 has a higher flame speed and a higher calorific value when compared to the other gases present in the syngas [26].

A study that focuses on the laminar flame speed of hydrogen/carbon monoxide/air mixtures determined that the laminar flame speed of an H_2/CO/air mixture increases with H_2 fraction [37]. A higher flame speed arising from the increased hydrogen content could potentially force the flame near the crevice regions [18] thus reducing the CO content present from incomplete combustion in the exhaust gases. Hence as the H_2 content and the H_2/CO ratio of the three syngas varies, the brake thermal efficiency and specific energy consumption data were cross compared across the three syngas blends.

Cross comparison of the brake thermal efficiency data showed that at full load there was no discernable difference between the performance of the syngas blends at all *% GEFs*.

The higher hydrogen content of SGC did not result in higher BTE values in comparison to the other syngas blends being evaluated at full engine load, this could be due to the fact that the combustion temperature is high enough at the full load to mitigate the effect of the slow burning rate of CO. At ~54% load, SGA had marginally higher brake thermal efficiency data and corresponding lower specific energy consumption values. At 30% load, there was no discernable difference between the brake thermal efficiency and the specific energy consumption data between the three gases. *(This data is not presented in this paper due to the page limit).*

However, at ~76% engine load, SGC had the higher brake thermal efficiency and lower corresponding specific energy consumption values at all *% GEFs*. The brake thermal efficiency comparison for the syngas blends at 76% engine load is shown in Figure 4.

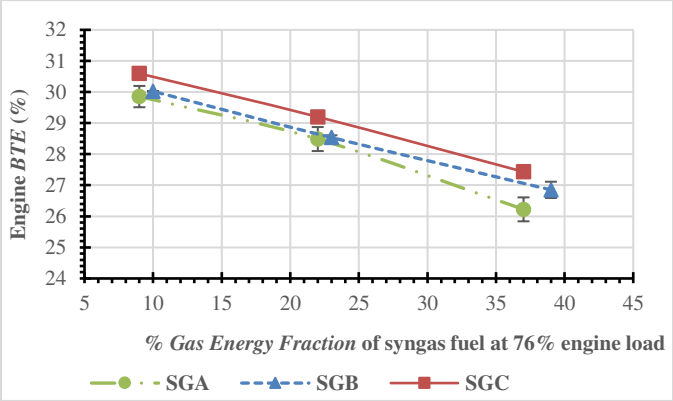

Figure 4. Cross comparison of *Brake Thermal Efficiency (BTE)* data at 76% engine load across syngas blends

The same brake thermal efficiency data at 76% load was expressed as a function of the hydrogen content in the syngas, and this is depicted in Figure 5.

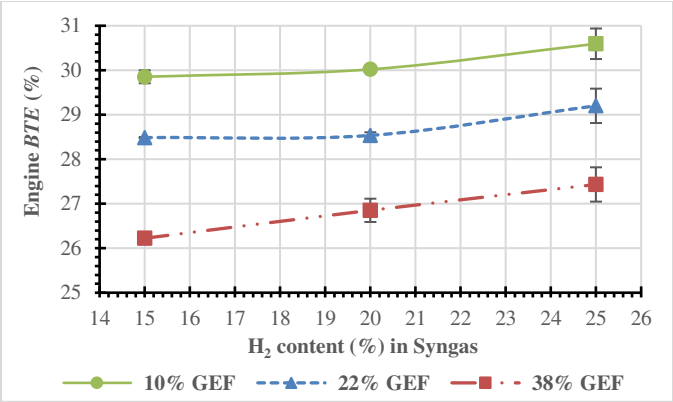

Figure 5. Cross comparison of the *% Brake Thermal Efficiency (BTE)* data versus H_2 content at 76% engine load

Thus, from Figure 5, it can be said that the hydrogen content of the syngas has an impact on the brake thermal efficiency, and the *GEF* value of 38% is more sensitive to changes in the hydrogen content of the syngas, as the brake thermal efficiency values change more dramatically when compared to 10 or 22%.

This is potentially due to the higher syngas flow used, thereby increasing the H_2 content of the syngas/air mixture. For ref, at ~76% load, diesel baseline data produced an average brake thermal efficiency value of 30.9%.

As mentioned in the introduction, a higher hydrogen content of syngas is said to promote fuller combustion. Hence to explain the higher brake thermal efficiency values seen for SGC in comparison to the other blends at 76% load, other parameters such as the P_{max}, *ID*, HC, and CO emissions were looked at to see if they supported the observed increase in brake thermal efficiency.

This study showed that the *ID* increased with increasing *% GEF* across every load for all three syngas blends relative to DBL data. These findings are corroborated by studies in the literature whereby many researchers have reported an increase in the *ID* with increasing substitution of syngas when in dual-fuel mode [6, 14, 20]. The increase in *ID* was more profound at higher loads ≥70%. Figure 6 illustrates the increase in *ID* with increasing syngas fraction across higher engine loads for SGB-diesel. Similar trends were observed for the other syngas blends.

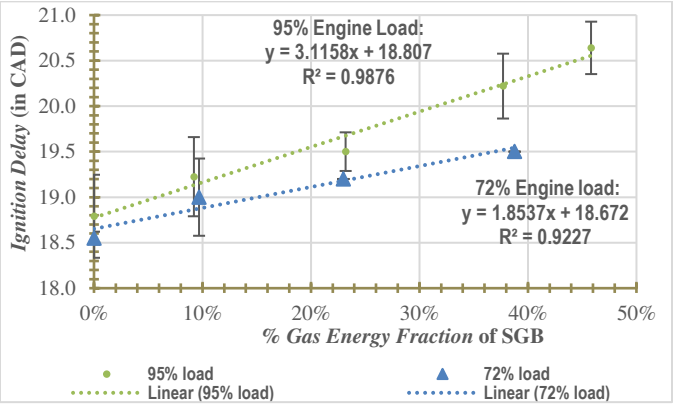

Figure 6. The *ID* at high engine loads versus the *% GEF* of SGB

The increase in *ID* can be explained by the fact that the addition of syngas into the cylinder is causing a delay in the auto-ignition of the pilot diesel fuel [6]. This increase in *ID* is due to the syngas-diesel dual fuel operation having a lower energy release rate versus diesel [13]. The late *ID* results in the combustion shifting into the expansion stroke thus causing a decrease in P_{max} in dual fuel mode. The P_{max} value is typically said to decrease when in dual-fuel mode versus pure diesel [6, 13, 30]. This experimental work confirmed that as the *% GEFs* increased, the P_{max} values decreased at all loads (except for full load using 46% *GEF* when using SGC where a minor increase was noted). Also, the location of P_{max} location (in terms of CAD) increased or was delayed; shifted away from the top dead centre (TDC) for all syngas blends at all *% GEF* values across all loads (versus diesel baseline). A longer *ID* shifts the P_{max} location away from TDC, towards the expansion stroke resulting in a reduction of cylinder peak pressure [13, 14]. Furthermore, the reduction in P_{max} seen can be explained further as the syngas is added, a concurrent reduction in the air supply is experienced. This decreases the air quantity induced causing a reduction in peak pressure [30].

The P-CAD data for SGB which illustrates the reduction in P_{max} and the shift in P_{max} location at full load is illustrated in Figure 7 which is representative of that seen for other syngas blends and testing loads/conditions (apart from one datapoint at full load, using 46% *GEF* for SGC as mentioned earlier).

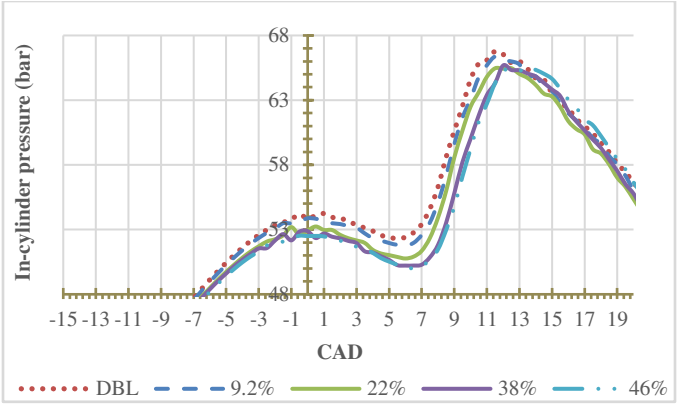

Figure 7. P-CAD dataset for SGB-diesel at full engine load at various gas energy fractions (*% GEF*s)

In summary, for all gas/diesel blends tested, the *ID* and P_{max} location increased, whilst P_{max} decreased with increasing *% GEF* at all loads relative to DBL data. These changes were more noticeable at higher loads than at lower loads. The increase in *ID* is caused by the alteration of the air/fuel ignition properties. Also, the low cetane number of the syngas fuels tested contributed to the longer *ID*, which became more profound as the *% GEF* increased [6].

The % change in the average P_{max} was calculated for the value obtained at the maximum *GEF* tested at that load, relative to DBL data. This cross comparison was carried out to determine if the syngas composition affected the P_{max} value as shown in Table 7.

Table 7. The % change in the P_{max} data (relative to DBL) per syngas blend

% Change in P_{max} (relative to DBL) for:	**SGA**	**SGB**	**SGC**
46% *GEF* at full load	-4.63	-1.70	2.63
38% *GEF* at 76% load	-5.43	-5.79	-2.25
22% *GEF* at 54% load	-2.24	-2.03	-3.29
22% *GEF* at 30% load	-1.74	-1.87	-0.57

In dual fuel combustion, the heat release rate study using SGA reported that as the gas fractions were increased, the heat release profiles shifted to the right (in CAD) as a result of changing combustion characteristics due to a decrease in the tendency of the dual fuel to ignite, leading to longer injection delays [6]. Hence when comparing this to SGB, and SGC, it can be said that the decrease in the *ID* seen in SGC relative to the other syngas bends can be attributed to the higher hydrogen content of the syngas. This results in a faster flame speed, which promotes more homogeneous combustion thus reducing ignition delay.

This HRR study for SGA dual fuel combustion also reported a reduction in the peak pressure and peak temperature relative to the diesel baseline [6]; the decrease in peak temperature was due to a reduction in the flame temperature. Also, Kousheshi et al. [18] reported that the P_{max} values increase with an increasing hydrogen content of the syngas. Thus, when considering these facts, when comparing the results for % change in P_{max} values reported in Table 7, the cause for SGC having the lowest change in P_{max} location versus the other syngas blends at engine loads >70% is a direct influence of its hydrogen content.

This data showed that SGC experienced the lowest % P_{max} drop/change at engine loads ≥ 70%, moreover, at full load, a pressure increase was seen relative to the diesel baseline. Overall, this confirms that the change in H_2 content enhanced affected the combustion performance at full and medium-high engine loads.

At lower engine loads (<56% engine load) the H_2/CO composition of the syngas has a reduced impact on the overall efficiency and combustion performance. Overall, these findings are consistent with that reported by other researchers [18, 36] who reported a decrease in the *ID*, an increase in P_{max}, local temperatures, and heat release, as the ratio of H_2 mass in the syngas was increased. Hydrogen rich mixtures are desired as they improve combustion efficiency.

For comparison, Figure 8 shows a comparison of the P_{max} values for the maximum *GEF* evaluated at full engine load across all three syngas blends. This clearly shows the impact of higher hydrogen content from the SGC plot.

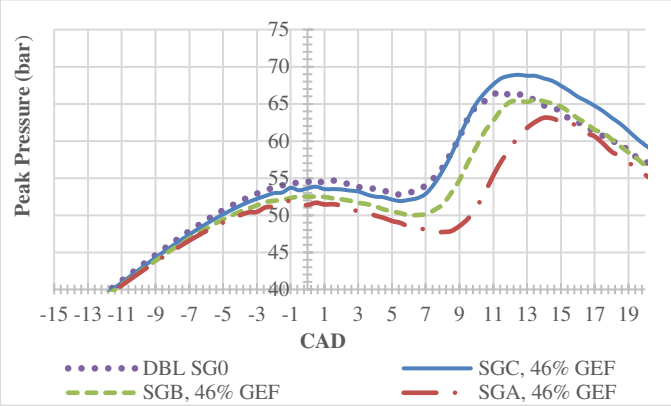

Figure 8. P-CAD profiles per syngas at full load at 46 % gas energy fraction

The change in the average P_{max} location data (expressed as CAD) derived from the P-CAD plots was cross-compared across gas types. The change in the CAD value of the P_{max} location was calculated by subtracting the P_{max} location (in CAD) at that test condition from the corresponding diesel baseline data. This data is shown in Table 8.

Table 8. The change in the P_{max} location in CAD (relative to DBL) per syngas

Change in P_{max} location in CAD (relative to DBL) for:	**SGA**	**SGB**	**SGC**
46% *GEF* at full load	2.25	1.50	0.95
38% *GEF* at 76% load	1.17	1.75	0.51
22% *GEF* at 54% load	0.33	1.00	0.45
22% *GEF* at 30% load	0.55	1.00	0.58

The comparison data in Table 8 shows that at higher engine loads (≥70%), SGC has the lowest change in P_{max} location versus the other syngas blends. At ~76% engine load, the SGC data shows a small marginal shift in the P_{max}. As discussed earlier, the higher H_2 content of this syngas, coupled with the higher H_2:CO ratio produces a smaller increase/shift of P_{max} value, hence the combustion rate of H_2 and CO is faster with more premixing being achieved. Also, this coupled with a smaller increase in *ID* sees a smaller shift of combustion phase into the expansion stroke (when compared to SGB/SGA) resulting in better combustion performance.

The increase in the *ID* (in CAD) data (was cross compared across gas types. This was done by calculating the % change in *ID* using the *ID* values from the diesel baseline and at the highest % *GEF* datapoint evaluated at each load; this is shown in Table 9. This data shows that at loads of ≥70%, SGC has the smallest increase in *ID* versus the other gaseous fuel types.

Table 9. The % change in the *ID* data (relative to DBL) per syngas

% Change in *ID* (relative to DBL) for:	**SGA**	**SGB**	**SGC**
46% *GEF* at full load	8.95	9.85	6.15
38% *GEF* at 76% load	7.26	5.12	4.41
22% *GEF* at 54% load	1.46	0.67	1.72
22% *GEF* at 30% load	1.67	0.72	-0.63

When looking at the effects of the hydrogen content of the syngas in dual fuel combustion, the literature reports that syngas blends containing higher hydrogen content had lower injection delays and higher peak pressure values than those with lower hydrogen content [17, 21]. Hence, a higher hydrogen content of syngas is said to promote fuller combustion.

Hence to summarise, at an engine load of ≥70%, SGC has the highest brake thermal efficiency, lowest specific energy consumption, the smallest decrease in peak pressure, the smallest shift in P_{max} location, and the smallest increase in *ID*, thus confirming this syngas has superior combustion performance at this load in comparison to the other syngas types evaluated.

Engine exhaust gas temperature

This study showed an increase in the engine exhaust gas temperature for all the syngas-diesel blends tested in dual fuel mode. This was attributed to a lack of adequate combustion time between diesel and syngas due to a longer *ID* [13] as shown in Table 9. Taking this temperature rise into consideration alongside the reduced brake thermal efficiency and P_{max}, increased specific energy consumption, and *ID* data, it can be said that the combustion performance is adversely affected (at every % *GEF* assessed) across all loads when using a syngas/diesel blend in dual-fuel mode versus pure diesel.

Engine exhaust gas temperatures were normalised against the exhaust gas temperature achieved for the diesel baseline and this data was cross compared across syngas blends. The normalised exhaust gas temperature plots for each load are illustrated in Figures 9 -12 (for engine loads of 96, 76, 54, and 30% respectively), whereby diesel baseline exhaust gas temperature represents 1.0. This comparison showed that at medium-high load engine loads (~76% engine load), SGC had marginally higher exhaust gas temperatures for all the *GEFs* evaluated. These findings can be explained by the fact that SGC has the highest hydrogen content versus SGA and SGB, this higher H_2 content has led to an increase in the average combustion temperature [30] thereby producing hotter exhaust gases, as seen by other researchers [14, 38]. The higher H_2 content increases the ignitability of the fuel, thus resulting in more stable combustion and higher efficiencies. This is due to the increased hydrogen content which enhances the lean limit of the mixture [36] and also produces a higher flame speed and temperatures [18], thereby improving combustion performance. The impact of hydrogen is potentially not observed at full load due to the existing high combustion temperatures. For the remaining loads, there was no noticeable difference in the change in temperature across the syngas blends evaluated.

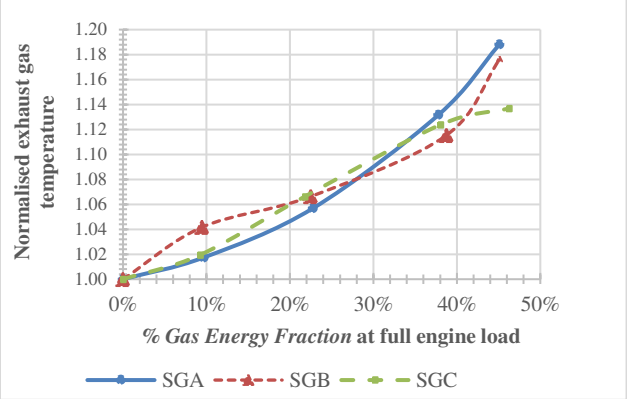

Figure 9. Exhaust gas temperature (normalised data) comparison for syngas blends at full engine load

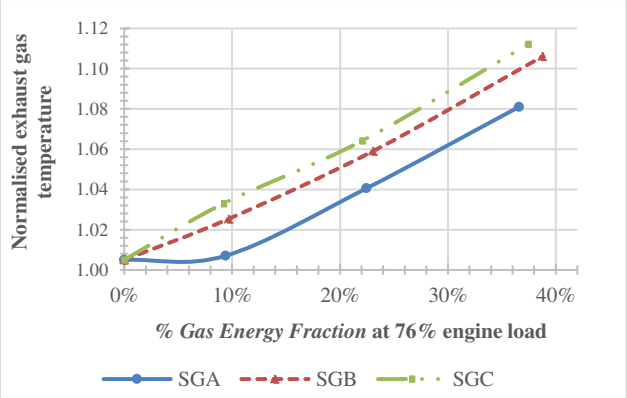

Figure 10. Exhaust gas temperature (normalised data) comparison for syngas blends at 76% engine load

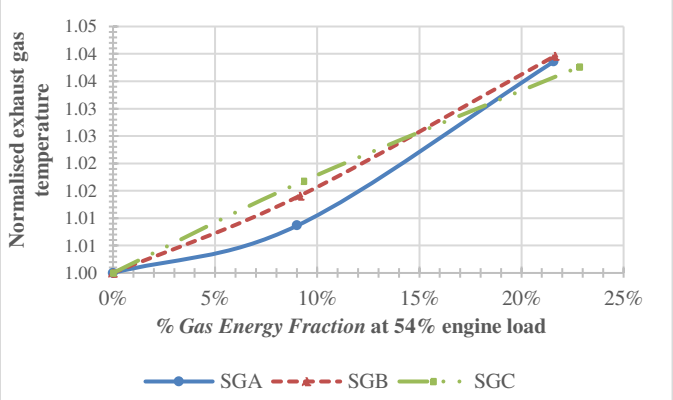

Figure 11. Exhaust gas temperature (normalised data) comparison for syngas blends at 54% engine load

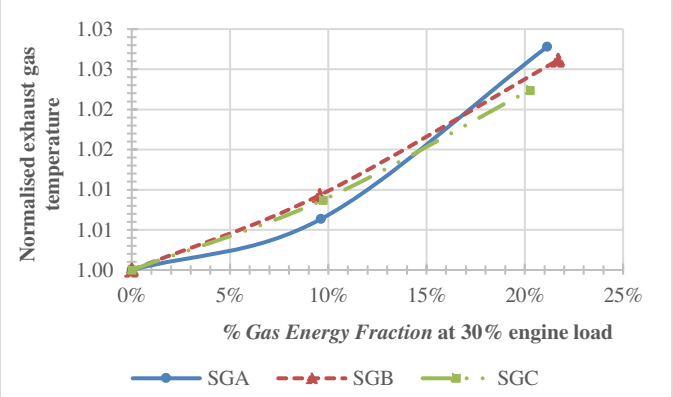

Figure 12. Exhaust gas temperature (normalised data) comparison for syngas blends at 30% engine load

Gaseous Emissions

The THC and CO levels both increased in dual fuel mode with increasing *% GEF*. The typical increases seen in the THC and CO *EI* data for dual fuel mode are depicted using Figures 13 and 14 using SGB-diesel, it was observed that SGA followed a similar trend. For SGC, a similar trend in THC and CO increase was seen, except for one data point. It was found that at full load, increasing the syngas fraction from ~38 to 46% did not significantly increase the CO or THC emissions for SGA and SGB, but for SGC this continued to increase. The increase in the CO data for SGC across all loads is depicted using Figure 15, the THC data for SGC follows a similar trend but is not shown in this paper. A similar trend in CO emissions was reported by Guo et al. [17] as discussed earlier whereby the CO levels did not increase further/significantly change after a certain point of syngas addition. The lack of change in the CO emissions at this point is potentially due to the limiting φ being reached**,** whereby the resulting CO and unburnt methane emissions are unaffected by the pilot diesel quantity. Badr et al. [39] reported that in dual fuel combustion, at low loads, the engine reaches an optimum or limiting equivalence ratio beyond which the CO and unburnt methane emissions remain unaffected by the pilot diesel quantity. It is stated that this point is a direct indication of the Φ limit for successful flame propagation from the pilot ignition centres [39].

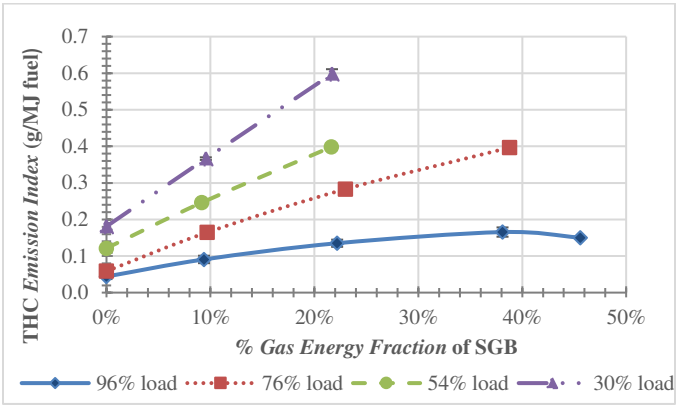

Figure 13. THC *Emission Index* data for SGB-diesel across various engine testing loads and at various *% GEF*s

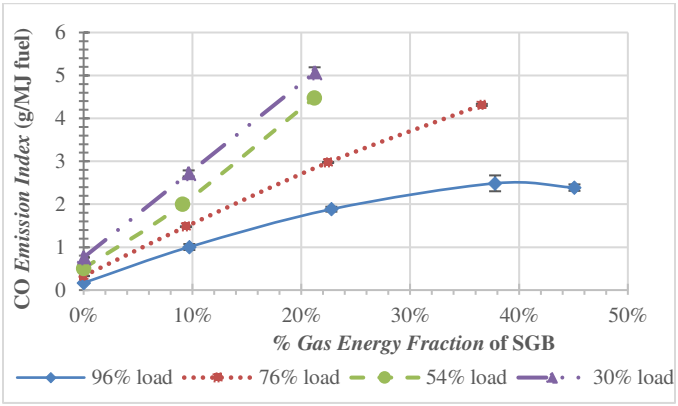

Figure 14. CO *Emission Index* data for SGB-diesel across various testing loads and at various *% GEF*s

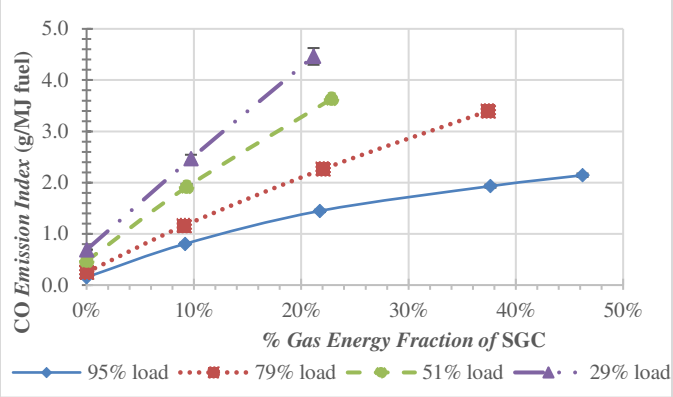

Figure 15. CO *Emission Index* data for SGC-diesel across various testing loads and at various % *GEF*s

In dual fuel mode, the contributing factors for the rise in CO emission include the lower energy content of the gas versus diesel, lower adiabatic flame temperatures (as seen for SGA [6]), and lower mean effective pressures [30]. For all gas-diesel blends, the THC and CO emissions observed in this study were significantly higher for loads < 56%. This was as expected as at lower loads dual-fuel engines are known for their lower thermal efficiency and higher unburned percentage of gaseous fuel [30], and similar findings have been reported by other researchers [15, 17, 30]. Also, at low loads, dual fuel engines have a longer combustion duration [6, 30], which leads to insufficient combustion time, resulting in incomplete combustion and raised emissions [14], as indicated by the lower engine exhaust gas temperatures.

In terms of CO emissions, in dual-fuel mode, incomplete combustion is most likely caused by a lower in-cylinder temperature which in turn is caused by a lower in-cylinder pressure [40]. The data for all gaseous blends also suggests that the CO and THC emissions are encouraged by a rich fuel mixture [30, 40]**.** In general, in this study, the THC emission values in dual fuel mode decreased as the load increased. This increase is due to higher combustion temperatures which enable oxidation of unburnt hydrocarbons [30], thereby reducing the THC emissions in the exhaust gases. For all dual-fuel bends tested**,** the typical trend seen was that as the % *GEF* increased the NO_x and NO decreased across all loads. This can be explained by the lower flame temperature and pressure, a lower rate of premixed combustion, and a reduction in the oxygen availability caused by the displacement of the air from the gas addition in dual-fuel mode versus diesel [6, 30, 41]. The trend in the NOx decrease is shown in Figure 16 for all gas blends at 76% load. Similar trends were noted for the remaining loads but are not shown in this paper.

It was noted by Sahoo et al. [13] that a larger % NO_x reduction (based on direct ppm emissions) was observed at lower engine loads (20 to 60%) with syngas-diesel. Hence % NO_x reduction data from this study was calculated based on diesel baseline and 23% *GEF* data across all loads using *EI* (in g/MJ) data. The % NO_x reductions did mirror the findings as reported by Sahoo et al.[13] for SGA only where optimum % NO_x reductions were achieved at ~54 % engine load. For SGB, the optimum % NO_x reductions were achieved at ~76% engine load (3kW), and SGC, at 30% load. Hence the % NO_x reductions for syngas-diesel combustion were found to be dependent on the syngas composition in this study. At ≤56% engine loads, for all syngas-diesel blends tested, typically the NO_2 concentration and the NO_2/NO_x ratio increased as % *GEF* increased.

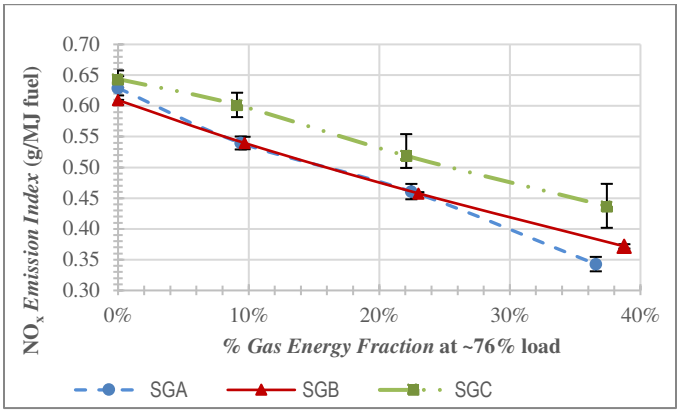

Figure 16. NO_x *Emission Index* data for the syngas fuels at 76% engine load at various % *GEF*s

Cross comparison of gaseous emissions.

The THC, CO, NO_x, and CO_2 emissions were cross compared using *EI* data (in g/MJ fuel). The graphs showing the comparison of the THC, CO, and NO_x emissions for ~76% load are shown in Figures 17 to 19, respectively.

Cross comparison data showed that the syngas with the highest H_2 content (SGC) had the cleanest combustion with respect to THC and CO emissions, which were lower at all loads assessed (relative to the other syngas fuels). Figure 17 illustrates this THC trend at 76% load. (Similar trends were noted at the remaining loads whereby SGC produced lower THC emissions relative to the other syngas blends, these trends are not shown in this paper due to the page limit). The engine combustion data (as discussed earlier), also supports that SGC should result in the lowest THC emissions, especially at high loads (≥70% engine load), SGC is associated with higher *brake thermal efficiency*, (specifically at 76% load), also, with the lowest increase in the value of *ID*, the highest P_{max}, and the smallest shift in P_{max} location, coupled with the highest engine exhaust gas temperatures (v SGA and SGB). All such conditions help promote better combustion and promote oxidation of UHCs, thus reducing the THCs found in the exhaust gases. At loads ≤56%, the reason for SGC having the lowest THC levels relative to the other syngas types is unclear. This is not directly evident by better engine combustion performance. However, this is possibly linked to its composition (higher H_2 content and H_2/CO ratio. Sahoo et al. [14] state that there is a minor impact of the H_2/CO composition on the thermal efficiency at part engine loads whereby

part-loads were identified as <40%. Further work is needed to determine the cause of this.

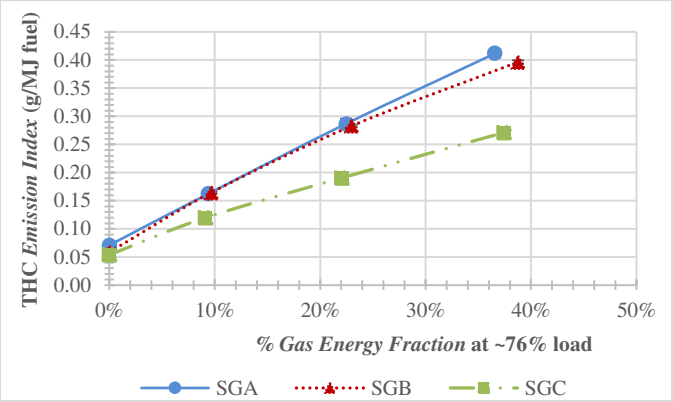

Figure 17. THC *Emission Index* data for the syngas fuels evaluated at 76% engine load

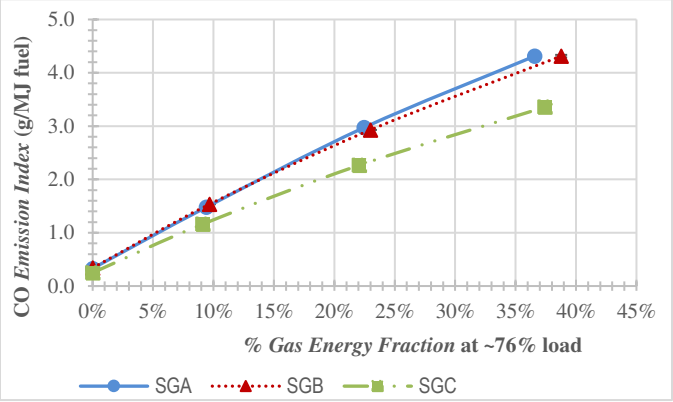

Figure 18. CO *Emission Index* data for the syngas fuels at 76% engine load at various *% GEFs*

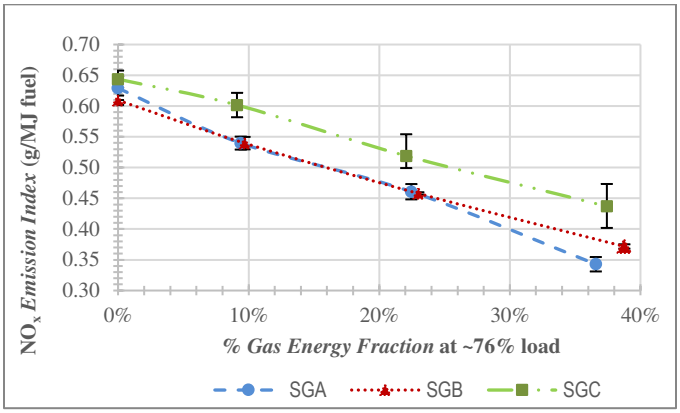

Figure 19. NO_x *Emission Index* data for the syngas fuels at 76% engine load at various *% GEFs*

As the CO composition in each syngas did not change, rather, the hydrogen content was increased, therefore, any changes in the CO emission data are not due to the change in the CO composition of the syngas. This study showed that SGC had the lowest CO emissions at all loads in comparison to the other syngas blends evaluated, and this is illustrated using Figure 18 which shows the cross-comparison data of CO *EI* values (in g/MJ fuel) at ~76% load. (Similar trends were noted at the remaining loads whereby SGC produced lower CO emission relative to the other syngas blends, this data is not shown in this paper due to the page limit). The most logical explanation for SGC having the lowest CO emissions is the enhanced combustion efficiency caused by the higher H_2 content in SGC which leads to reduced CO emissions, as seen by other researchers [18, 36].

Also, CO emissions are boosted by fuel-rich mixtures. Of all syngas types evaluated, SGC has the highest LHV, therefore requiring lower flow rates to obtain the same energy content in comparison to SGA and SGB. Hence when using SGC, lower flow rates meant less displacement of air/oxygen, thus in theory this mixture was always leaner. In addition, the faster flame speed of hydrogen helps to burn the trapped CO within the crevices of the combustion chamber thus helping to reduce CO emissions [18]. Consequently, a combination of these effects leads to cleaner combustion in terms of CO and HC emissions.

Cross-comparison of the NO_x *EI* data indicated that SGC has the highest NO_x values at loads ≥~70%. The cross-comparison data for 76% load is illustrated in Figure 19, and the trend seen for full load is similar (although it is not shown in the paper). The higher H_2 content of SGC leads to higher NO_x emissions, other findings in the literature support this whereby higher NO_x emissions have been reported for fuels with higher H_2 content due to higher in-cylinder pressure and combustion temperatures [14, 18, 36, 38].

As discussed earlier, SGC also had higher in-cylinder pressures (at loads ≥~70%), and higher engine exhaust gas temperatures for SGC (at an engine load of 76%), relative to the rest of the syngas types, which indicate higher combustion temperatures, thus confirming these findings. However, for lower loads (≤56% engine load), the higher H_2 content of the syngas does not appear to result in higher NO_x values as SGC does not produce the highest NOx emissions in comparison to the other syngas blends. One plausible explanation for this is that at these load conditions the benefits of the faster flame velocity of H_2 are lost due to the lower combustion temperatures. Instead, SGB (which contains equal amounts of H_2/CO or a 1:1 ratio) produced the highest NO_x levels. CO_2 emissions are not reported in the paper. However, it was observed that in dual fuel mode, for all syngas blends, at loads ≥70%, as the syngas fraction increased so did the resulting CO_2 emissions. There was no discernable difference between the CO_2 emissions produced from each of the syngas blends assessed at these loads.

Particle number emissions

This study showed that the TPNC (cm^3) decreased with increasing syngas addition at full, 76%, and 54% loads for all syngas-diesel blends tested; the diesel baseline had the highest TPNC. The TPNC at each *% GEF* for each load is summarised for each syngas blend in Table 10. This reduction in TPNC in dual fuel mode was due to the decrease in diesel consumption, thereby resulting in lower particulates. The reduced diesel consumption resulted in fewer pyrolysis of diesel fuel in the diffusing combustion phase and thus led to lower particulate emissions. At 30% load, an increase was noted in the TPNC as the *% GEF* increased for all syngas blends tested, this was thought to be due to reduced thermal efficiency and more incomplete combustion at this load.

Table 10. The TPNC data per *GEF* for each syngas blend per load

% Load		SGA	SGB	SGC
	% *GEF*	TPNC		
96	**0**	1.19E+08	1.12E+08	1.10E+08
	9.5	1.13E+08	1.09E+08	9.64E+07
	22	1.10E+08	1.01E+08	1.01E+08
	38	1.03E+08	8.54E+07	9.73E+07
	46	9.93E+07	9.11E+07	9.62E+07
76	**0**	1.03E+08	8.74E+07	9.38E+07
	9.5	9.60E+07	8.39E+07	8.58E+07
	22	7.71E+07	7.06E+07	8.01E+07
	38	5.78E+07	4.98E+07	6.27E+07
54	**0**	1.00E+08	8.95E+07	9.48E+07
	9.5	9.09E+07	8.18E+07	7.72E+07
	22	6.32E+07	7.42E+07	6.00E+07
30	**0**	8.92E+07	2.29E+08	6.11E+07
	9.5	1.10E+08	3.13E+08	3.22E+08
	22	1.16E+08	5.08E+08	3.25E+08

The % change in the TPNC was calculated between the value obtained at the maximum *GEF* tested at that load, relative to DBL data. and this is summarised for all syngas blends in Table 11. The TPNC data was not cross compared due to slight variations in the engine testing load conditions which would affect the comparison data.

Table 11. The % change in the TPNC data (relative to DBL) per syngas

% Change in TPNC (relative to DBL) for	SGA	SGB	SGC
46% *GEF* at full load	-17%	-18%	-12%
38% *GEF* at 76% load	-44%	-43%	-33%
22% *GEF* at 54% load	-37%	-17%	-37%
22% *GEF* at 30% load	+30%	+122%	+432%

The PSD profiles were compared per load with increasing syngas addition for each dual fuel. At loads ≥70%, no noticeable change in the PSD profile was observed for any of the syngas blends tested. Also, at full load, there was no obvious trend /order apparent in terms of correlation to % syngas added versus decrease in particle number concentration. However, for 76% load, there is a clear trend whereby a reduction in the particle number concentration is seen with a corresponding reduction in diesel usage and/or increasing the syngas fraction.

Figures 20 and 21 show the PSD curves for full and 76% load at the various % *GEFs*; these graphs show a reduction in the particle number concentration with no change in the PSD. It is observed that the trend in particle concentration reductions with % *GEF* is less clear at the full load (Figure 20) than those at the lower loads such as Figures 21 and 22. This is likely to be that at the full load condition, syngas fractions were not a dominant factor anymore for the formation of particles. In other words, the effect of syngas on particle reduction decreased.

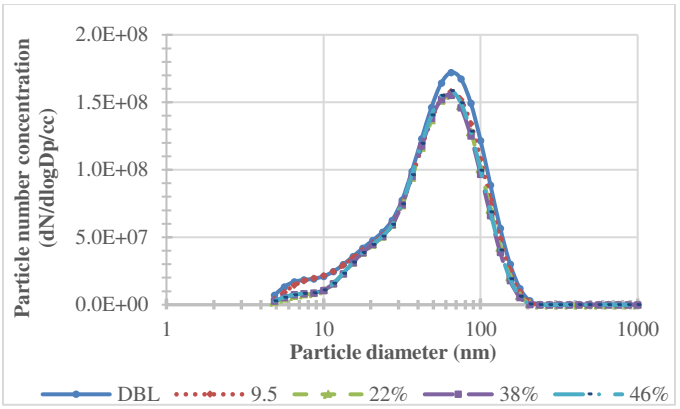

Figure 20. PSD curves at full engine load for SGB-diesel at 0, 9.5, 22, 38, and 46% gas energy fractions (% *GEF*s)

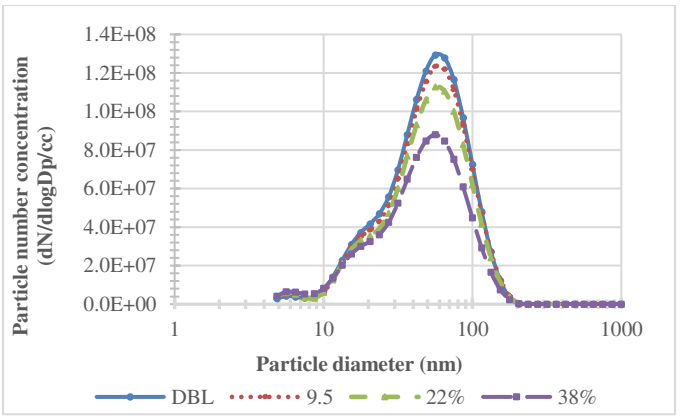

Figure 21. PSD curves at 76% load for SGC-diesel at 0, 9.5, 22, and 38% gas energy fractions (% *GEF*s)

For all dual fuel blends at 54% engine load, the PSD changed: the particle number concentration related to accumulation mode decreased while the nucleation mode increased. This bimodal trend is similar to that reported by Chuahy et al. [24]. The change in the PSD at 54% engine load for SGB is illustrated using Figure 22. This is similar to that observed for SGA and SGC at this testing load (these graphs are not shown in this paper).

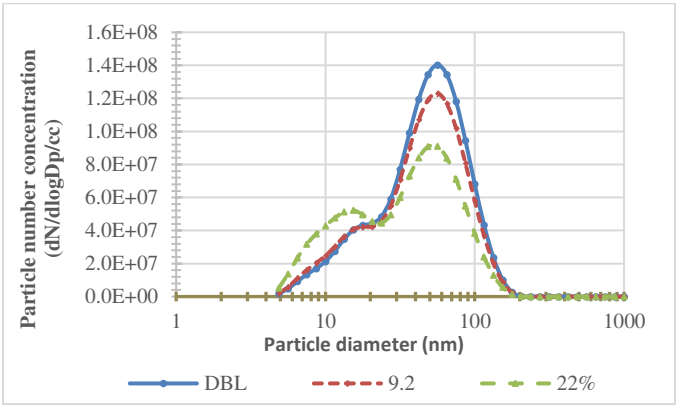

Figure 22. PSD curves at 54% load for SGB-diesel at 0, 9, and 22% gas energy fractions *(% GEFs)*

However, at engine loads of 30%, the changes noted in the PSD are dependent on the syngas blends. For SGA, at 30% load, the change in the PSD profile with syngas addition is similar to the trend observed at 54% engine load whereby an increase is seen in the particle concentration number for the nucleation mode and a reduction in the accumulation mode.

The change in the PSD at 30% engine load for SGA is illustrated using Figure 23. However, for SGB and SGC, at an engine load of 30%, a change is seen in the PSD, however, it is difficult to compare this trend within the PSD curve due to the loss of the bimodal distribution with syngas addition. The PSD curve for SGB at 30% engine load is shown in Figure 24, and for SGC, this is shown using Figure 25.

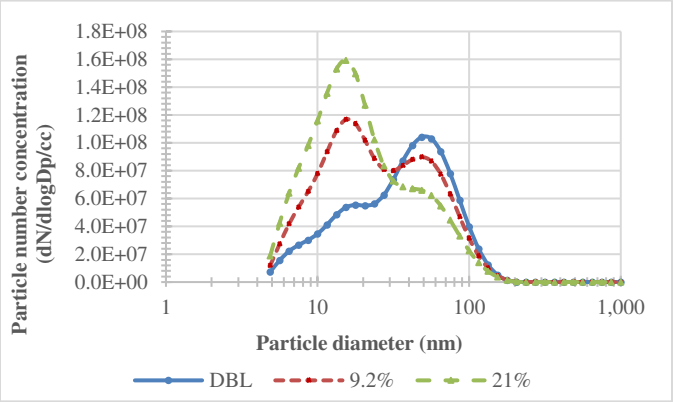

Figure 23. PSD curves at 30% load for SGA-diesel at 0, 9.2, and 22% gas energy fractions *(GEFs)*

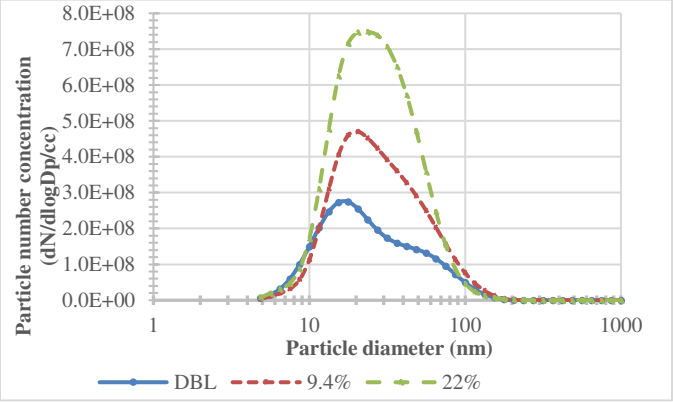

Figure 24. PSD curves at 30% load for SGB-diesel at 0, 9.4, and 22% gas energy fractions *(GEFs)*

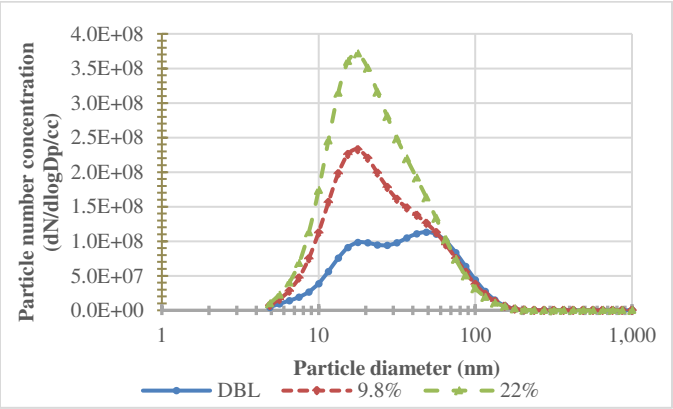

Figure 25. PSD curves at 30% load for SGC-diesel at 0, 9.8, and 22% gas energy fractions *(GEFs)*

Limited particle emissions data has been reported in this paper. The PM mass data arising from syngas-diesel dual fuel combustion at high engine load using 10 and 22% *GEF*s from this study have been investigated in full detail and will be reported in a later paper.

A summary of the combustion performance of SGC

Thus, in summary, SGC presented with superior combustion performance, the supporting data for this include:

- Highest *BTE* value and lowest *SEC* data at ~76% engine load
- The smallest decrease in P_{max} at engine loads ≥70%
- The smallest increase in *ID* at engine loads ≥70%
- The smallest delay in P_{max} location at engine loads ≥70%
- Highest exhaust gas temperature at 76% engine load
- Lowest THC and CO emissions across all engine loads and % *GEF*s.
- Highest NO_x emissions at engine loads ≥70%

Thus, the performance and emissions arising from the maximum % *GEF* at full and 76% load were compared for SGC to determine which is most beneficial. Parameters such as the brake thermal efficiency, the mass diesel displacement ratio, % change in TPNC, and % change in *SE* emissions were compared relative to the diesel baseline. Also, reductions in CO_2 emissions arising directly from the reduction in diesel consumption in dual fuel mode were calculated using experimental diesel consumption data. The kg CO_2 produced was based on the assumption that 1 litre of red diesel produces ~2.7kg of CO_2 [42]. The comparison is summarised in Table 12.

Table 12. Emission and performance comparison of two testing conditions using SGC in dual fuel mode

Parameter	**46% *GEF* at full load.**	**38% *GEF* at 76% load**
BTE %	27.1	27.4
SEC (MJ/kWh)	13.3	13.1
ϕ	0.60	0.48
Diesel replacement rate %	39%	28%
% Change in TPNC	-12	-23
% $CO_{2\ eq}$ kg reduction	39	28
% Change in THC *SE*	+353	+534
% Change in CO *SE*	+1462	+1452
% Change in NO_x *SE*	-16	-26

The data in Table 12 suggests that in terms of diesel displacement, the corresponding reductions in CO_2 equivalent emissions, and the THC emissions, running at full load using a syngas energy fraction of 46% is more beneficial than at 76% load using a *GEF* of 76%. However, running at 76% load using a *GEF* of 38% is more advantageous when considering the % TPNC, NO_x, and CO emissions reductions. The brake thermal efficiency data is comparable between the two datapoints.

Conclusions

In this work, three different simulated syngas blends were tested whereby the composition was based on that typically produced from a downdraft gasifier. The difference between the three syngas compositions was the varying hydrogen content with SGC having the highest (as well as the highest H_2/CO ratio).

The effects on the combustion performance and the resulting emissions were investigated at 30, 54, 76, and 96% engine load using various syngas fractions varying from 10 to 46% in a dual fuel RCCI enabled high-speed diesel genset 5.7kW engine. It was found that in dual fuel mode (relative to diesel baseline), for all the syngas blends tested, as the syngas fraction increased, the trends noted at all engine testing loads (unless specified) were:

- An increase in the engine exhaust gas temperature
- Longer *ID*, and higher *SEC*
- A reduction in *BTE* and P_{max}
- An increase/shift in the P_{max} location away from TDC
- An increase in the % mass of diesel displaced, a maximum diesel displacement value of ~39 % was achieved at full engine load using a gas energy fraction of 46%
- An increase in the THC and CO emissions
- A decrease in the NO_x and NO emissions
- An increase in NO_2 emissions and the NO_2/NO_x ratio at loads ≤56%
- A reduction in the TPNC with no change in the PSD curves for all engine loads except for 30%.
- At 30% engine load, the TPNC increased in dual fuel mode alongside a change in the PSD profile, the change noted was dependent on the syngas-blend.

The trends discussed earlier noted in dual fuel mode were a direct result of reduced combustion efficiency. When considering the differing syngas composition, it can be concluded that SGC presented superior combustion performance in dual fuel mode. This was primarily due to the higher H_2 content, which enhanced combustion performance in comparison to the other syngas blends evaluated.

Limited particle emissions data has been reported in this paper. The PM mass arising from syngas-diesel dual fuel combustion from this study has been investigated in full detail and will be reported in a later paper.

References

1. Zebra, C., Windt, H., Nhumaio, G., and Faaij, A., *A review of hybrid renewable energy systems in mini-grids for off-grid electrification in developing countries.* Renewable & sustainable energy reviews, 2021. **144**: p. 111036 DOI: 10.1016/j.rser.2021.111036.
2. Ahlborg, H. and Hammar, L., *Drivers and barriers to rural electrification in Tanzania and Mozambique – Grid-extension, off-grid, and renewable energy technologies.* Renewable Energy, 2014. **61**: p. 117-124 DOI: 10.1016/j.renene.2012.09.057.
3. Bertheau, P., Cader, C., Müller, H., Blechinger, P., Seguin, R., and Breyer, C., *Energy Storage Potential for Solar Based Hybridization of Off-grid Diesel Power Plants in Tanzania*. 2014, Elsevier Ltd. p. 287-293.
4. African Development Bank Group, *Renewable Energy in Africa: TANZANIA Country Profile*. 2015, Immeuble du Centre de commerce International d'Abidjan - CCIA: Côte d'Ivoire.
5. Aslam, Z., Li, H., Hammerton, J., Andrews, G., Ross, A., and Lovett, J., *Increasing Access to Electricity: An Assessment of the Energy and Power Generation Potential from Biomass Waste Residues in Tanzania.* Energies, 2021. **14**(6): p. 1793 DOI: 10.3390/en14061793.
6. Olanrewaju, F., Li, H., Aslam, Z., Hammerton, J., and Lovett, J., *Analysis of the effect of syngas substitution of diesel on the Heat Release Rate and combustion behaviour of Diesel-Syngas dual fuel engine.* Fuel, 2022. **312**: p. 122842 DOI: 10.1016/j.fuel.2021.122842.
7. Rinaldini, C.A., Allesina, G., Pedrazzi, S., Mattarelli, E., Savioli, T., Morselli, N., Puglia, M., and Tartarini, P., *Experimental investigation on a Common Rail Diesel engine partially fuelled by syngas.* Energy conversion and management, 2017. **138**: p. 526-537 DOI: 10.1016/j.enconman.2017.02.034.
8. Basu, P., *Biomass gasification and pyrolysis : practical design and theory*. 2010, Amsterdam ;: Elsevier/Academic Press.
9. Simonyan, K.J. and Fasina, O., *Biomass resources and bioenergy potentials in Nigeria.* African Journal of Agricultural Research, 2013. **8**(40): p. 4975-4989.
10. Terrapon-Pfaff, J.C., *Linking Energy- and Land-Use Systems: Energy Potentials and Environmental Risks of Using Agricultural Residues in Tanzania.* SUSTAINABILITY, 2012. **4**(3): p. 278-293 DOI: 10.3390/su4030278.
11. Liu, H., Tang, Q., Yang, Z., Ran, X., Geng, C., Chen, B., Feng, L., and Yao, M., *A comparative study on partially premixed combustion (PPC) and reactivity controlled compression ignition (RCCI) in an optical engine.* Proceedings of the Combustion Institute, 2019. **37**(4): p. 4759-4766 DOI: 10.1016/j.proci.2018.06.004.
12. Inagaki, K., Fuyuto, T., Nishikawa, K., Nakakita, K., and Sakata, I., *Dual-Fuel PCI Combustion Controlled by In-Cylinder Stratification of Ignitability*. 2006.
13. Sahoo, B.B., Sahoo, N., and Saha, U.K. *Assessment of a Syngas-Diesel Dual Fuelled Compression Ignition Engine*. in *ASME 2010 4th International Conference on Energy Sustainability*. 2010. DOI: 10.1115/es2010-90218.
14. Sahoo, B.B., Sahoo, N., and Saha, U.K., *Effect of H_2:CO ratio in syngas on the performance of a dual fuel diesel engine operation.* Applied thermal engineering, 2012. **49**: p. 139-146 DOI: 10.1016/j.applthermaleng.2011.08.021.
15. Bika, A.S., Franklin, L., and Kittelson, D., *Cycle Efficiency and Gaseous Emissions from a Diesel Engine Assisted with Varying Proportions of Hydrogen and Carbon Monoxide (Synthesis Gas).* 2011, SAE International.
16. Mahmood, H.A., Al-Sulttani, A.O., and Attia, O.H., *Simulation of Syngas Addition Effect on Emissions Characteristics, Combustion, and Performance of the Diesel Engine working under Dual Fuel Mode and Lambda Value of 1.6.*, in *IOP Conf. Series: Earth and Environmental Science*. 2021, IOP Publishing Ltd.
17. Guo, H., Neill, W.S., and Liko, B. *The Combustion and Emissions Performance of a Syngas-Diesel Dual Fuel Compression Ignition Engine*. 2016. American Society of Mechanical Engineers DOI: 10.1115/icef2016-9367.
18. Kousheshi, N., Yari, M., Paykani, A., Saberi Mehr, A., and De La Fuente, G.F., *Effect of Syngas Composition on the Combustion and Emissions Characteristics of a Syngas/Diesel RCCI Engine.* Energies, 2020. **13**(1): p. 212 DOI: 10.3390/en13010212.
19. Tuan, L.A. and Luong, H., *Simulation of a syngas - diesel dual fuel engine for small-scale power generator.* 2014. **100B**: p. 36-41.
20. Monorom, R., Bernard, B., Gitano-Briggs, H.W., and Jose Bienvenido Manuel, M.B., *Design and fabrication of a low-cost research facility for the study of combustion characteristics of a dual producer gas-diesel engine.* Engineering and Applied Science Research (EASR), 2020. **47**(4): p. 447-457 DOI: 10.14456/easr.2020.48.
21. Jamsran, N., Park, H., Lee, J., Oh, S., Kim, C., Lee, Y., and Kang, K., *Syngas composition for improving thermal efficiency in boosted homogeneous charge compression ignition engines.* Fuel (Guildford), 2022. **321** DOI: 10.1016/j.fuel.2022.124130.

22. Chuahy, F. and Kokjohn, S., *High efficiency dual-fuel combustion through thermochemical recovery and diesel reforming.* Applied energy, 2017. **195**: p. 503-522 DOI: 10.1016/j.apenergy.2017.03.078.
23. Dal Forno Chuahy, F., Olk, J., and Kokjohn, S., *Reformed Fuel Substitution for Transient Peak Soot Reduction*. 2018.
24. Chuahy, F., Strickland, T., Walker, R., N,, and Kokjohn, S., *Effects of reformed fuel on dual-fuel combustion particulate morphology.* International journal of engine research, 2021. **22**(3): p. 777-790 DOI: 10.1177/1468087419879782.
25. Ramadhas, A.S., Jayaraj, S., and Muraleedharan, C., *Power generation using coir-pith and wood derived producer gas in diesel engines.* Fuel Processing Technology, 2006. **87**(10): p. 849-853 DOI: 10.1016/j.fuproc.2005.06.003.
26. Feng, S., *Numerical Study of the Performance and Emission of a Diesel-Syngas Dual Fuel Engine.* Mathematical problems in engineering, 2017. **2017**: p. 1-12 DOI: 10.1155/2017/6825079.
27. Hernández, J.J., Ballesteros, R., Barba, J., and Guillén-Flores, J., *Effect of the Addition of Biomass Gasification Gas on the PM Emission of a Diesel Engine.* SAE International Journal of Engines, 2014. **8**(1): p. 14-19 DOI: 10.4271/2014-01-2840.
28. Hernández, J.J., Lapuerta, M., and Barba, J., *Effect of partial replacement of diesel or biodiesel with gas from biomass gasification in a diesel engine.* Energy (Oxford), 2015. **89**: p. 148-157 DOI: 10.1016/j.energy.2015.07.050.
29. Uma, R., Kandpal, T.C., and Kishore, V.V.N., *Emission characteristics of an electricity generation system in diesel alone and dual fuel modes.* Biomass & bioenergy, 2004. **27**(2): p. 195-203 DOI: 10.1016/j.biombioe.2004.01.003.
30. Sahoo, B.B., Sahoo, N., and Saha, U.K., *Effect of engine parameters and type of gaseous fuel on the performance of dual-fuel gas diesel engines—A critical review.* Renewable & sustainable energy reviews, 2009. **13**(6): p. 1151-1184 DOI: 10.1016/j.rser.2008.08.003.
31. Crown Oil. *EN 590 Diesel Fuel Specifications (ULSD)*. 2022 [cited 2022 16th Feb 22]; Available from: https://www.crownoil.co.uk/fuel-specifications/en-590/.
32. Alagumalai, A., *Combustion characteristics of lemongrass (Cymbopogon flexuosus) oil in a partial premixed charge compression ignition engine.* Alexandria Engineering Journal, 2015. **54**(3): p. 405-413 DOI: 10.1016/j.aej.2015.03.021.
33. Silvis. M, W., *The Algorithmic Structure of the Air/Fuel Ratio Calculation*, in *Readout No 15*, H.T. Reports, Editor. 1997. p. 17-24.
34. Li, H., Ropkins, K., Andrews, G.E., Daham, B., Bell, M.C., and Tate, J.E., *Evaluation of a FTIR Emission Measurement System for Legislated Emissions Using a SI Car*. 2006: Society of Automotive Engineers.
35. Sahoo, B.B., Saha, U.K., and Sahoo, N., *Theoretical performance limits of a syngas–diesel fueled compression ignition engine from second law analysis.* Energy (Oxford), 2011. **36**(2): p. 760-769 DOI: 10.1016/j.energy.2010.12.045.
36. Azimov, U., Tomita, E., Kawahara, N., and Harada, Y., *Effect of syngas composition on combustion and exhaust emission characteristics in a pilot-ignited dual-fuel engine operated in PREMIER combustion mode.* International journal of hydrogen energy, 2011. **36**(18): p. 11985-11996 DOI: 10.1016/j.ijhydene.2011.04.192.
37. Dong, C., Zhou, Q., Zhao, Q., Zhang, Y., Xu, T., and Hui, S., *Experimental study on the laminar flame speed of hydrogen/carbon monoxide/air mixtures.* Fuel (Guildford), 2009. **88**(10): p. 1858-1863 DOI: 10.1016/j.fuel.2009.04.024.
38. Mohon Roy, M., Tomita, E., Kawahara, N., Harada, Y., and Sakane, A., *Performance and emission comparison of a supercharged dual-fuel engine fueled by producer gases with varying hydrogen content.* International journal of hydrogen energy, 2009. **34**(18): p. 7811-7822 DOI: 10.1016/j.ijhydene.2009.07.056.
39. Badr, O., Karim, G.A., and Liu, B., *An examination of the flame spread limits in a dual fuel engine.* Applied thermal engineering, 1999. **19**(10): p. 1071-1080 DOI: 10.1016/S1359-4311(98)00108-2.
40. Wagemakers, A.M.L.M. and Leermakers, C.A.J., *Review on the Effects of Dual-Fuel Operation, Using Diesel and Gaseous Fuels, on Emissions and Performance*. 2012.
41. Rößler, M., Koch, T., Janzer, C., and Olzmann, M., *Mechanisms of the NO2 Formation in Diesel Engines.* MTZ worldwide, 2017(7-8).
42. U.K. Department for Business, E.I.S. *Greenhouse gas reporting: conversion factors 2021*. 2021 [cited 2022 April]; Available from: https://www.gov.uk/government/publications/greenhouse-gas-reporting-conversion-factors-2021.

Contact Information

Zahida Aslam
School of Chemical and Process Engineering, (ScaPE)
University of Leeds.
Email: pmzba@leeds.ac.uk
Tel.: +44 7737 072730

Acknowledgments

This research was possible due to the financial aid by The Engineering and Physical Sciences Research Council (EPSRC) for a PhD studentship for Zahida Aslam in the Centre for Doctoral Training in Bioenergy (EP/L014912/1), and a GCRF grant: Creating resilient sustainable micro-grids through hybrid renewable energy systems (CRESUM-HYRES), grant number EP/R030243/1. We also appreciate and acknowledge Mr. Scott Prichard for his technical support and expertise.

Definitions/Abbreviations

AFR_{DBL}	Air to Fuel Ratio for diesel baseline
AFR_{df}	Air to Fuel Ratio for dual fuel
$AFR_{stoic\text{-}diesel}$	Stoichiometric air to flow ratio of diesel
$AFR_{stoic\text{-}diesel}$	Stoichiometric air to flow ratio of diesel
BP	Engine brake power output
BMEP	Brake Mean Effective Pressure
bTDC	Before Top Dead Centre
BTE	Brake Thermal Efficiency

$\boldsymbol{\theta}$	Crank Angle Degree
CAD	Crank Angle Degree
$\mathbf{C_i}$	Concentration of a gaseous pollutant
cc	Cubic centimeters
CN	Cetane Number
DBL	Diesel baseline
$\boldsymbol{DoC}$	Duration of combustion
$\boldsymbol{EI}$	Emission Index
EGR	Exhaust Gas Recirculation
$\boldsymbol{\phi_{DBL}}$	Equivalence ratio for diesel baseline
$\boldsymbol{\phi_{df}}$	Equivalence ratio for dual fuel mode
$\boldsymbol{GEF}$	Gas energy fraction
$\boldsymbol{HRR}$	Heat Release Rate
$\boldsymbol{ID}$	Injection delay
$\mathbf{IMEP_n}$	Net Indicated Mean Effective Pressure
$\mathbf{k_{gas}}$	Conversion coefficient of the gaseous pollutant
kW	Kilowatt
$\boldsymbol{LHV_d}$	Lower Heating Value of diesel
$\boldsymbol{LHV_{df\ blend}}$	LHV of the pilot diesel and syngas
$\boldsymbol{LHV_g}$	Lower Heating Value of syngas
$\boldsymbol{m_{DF\ air}}$	Mass of air intake in dual fuel mode
$\boldsymbol{m_{DBL\ air}}$	Mass of air intake in pure diesel mode
$\boldsymbol{m_d}$	Mass flow rate of diesel used for diesel baseline
$\boldsymbol{m_g}$	Mass flow rate of syngas
$\boldsymbol{m_{pd}}$	Mass flow rate of pilot diesel in dual fuel mode
$\mathbf{P_{max}}$	Maximum/peak Pressure
P-CAD	Pressure – crank angle degree
PM	Particulate matter
PoHRR	Peak of heat release rate
PSD	Particle Size Distribution
RCCI	Reactivity Controlled Compression Ignition
RPM	Revolutions Per Minute
$\boldsymbol{SE}$	Specific Emission
$\boldsymbol{SEC_{df}}$	Specific energy consumption in dual fuel mode
$\boldsymbol{SFC}$	Specific Fuel Consumption
SGA	Syngas A
SGB	Syngas B
SGC	Syngas C
SoC	Start of Combustion
SoI	Start of Injection
TDC	Top Dead Centre
THC	Total Hydrocarbons
TPNC	Total Particle Number Concentration
ULSD	Ultra-Low Sulphur Diesel
UHC	Unburnt Hydrocarbons
Z	Diesel displacement ratio

Appendix

The % Gas Energy Fraction (*GEF*) substitution value was calculated using Eq. (A1). Here**,** m_g is the mass flow rate of the syngas, kg/h, LHV_g is the calculated LHV for the syngas, MJ/kg, LHV_d is the LHV of diesel, MJ/kg, and m_{pd} is the mass flow rate of pilot diesel in dual fuel mode, kg/h.

$$GEF\ (\%) = \frac{(\boldsymbol{m_g\ x\ LHV_g})}{(\boldsymbol{m_{pd} x\ LHV_d + m_g\ x\ LHV_g})} \quad \text{(A1)}$$

The *ID* was calculated in crank angle degree (CAD) using Eq. (A2). Here, *ID* is the ignition delay, CAD, *SoC* is the start of combustion, CAD, and *SoI* is the start of injection which is 13.5 CAD before the top dead centre (bTDC).

$$ID\ (CAD) = SoC\ (CAD) + SoI\ (13.5\ \Theta\ bTDC) \quad \text{(A2)}$$

The Specific Fuel Consumption (*SFC* in g/kWh) for diesel baseline was calculated using Eq. (A3), where m_d is the mass flow rate of diesel for diesel baseline, g/h, and *BP* is the engine brake power output, kW.

$$SFC\ = \left(\frac{m_d}{BP}\right) \quad \text{(A3)}$$

The Specific Energy Consumption for dual fuel mode (SEC_{df}) in MJ/kWh Eq. (A4), where m_{pd} is the mass flow rate of pilot diesel in dual fuel mode, kg/h, LHV_g is the calculated LHV for the syngas, MJ/kg, m_g is the mass flow rate of the syngas, kg/h, LHV_d is the LHV of diesel, MJ/kg, and *BP* is the engine brake power output, kW

$$SEC_{df} = \frac{(m_{pd}\ x\ LHV_d) + (m_g\ x\ LHV_g)}{BP} \quad \text{(A4)}$$

The Brake Thermal Efficiency (*BTE*) for dual fuel mode was calculated using Eq. (A5) and the *BTE* for diesel baseline was calculated using Eq. (A6), where m_{pd} *is* the mass flow rate of pilot diesel in dual fuel mode, kg/s, m_d is the mass flow rate of diesel for diesel baseline, kg/s, m_g is the mass flow rate of syngas, kg/s, *BP* is the engine brake power output, kW, LHV_d is the LHV of diesel, KJ/kg, and LHV_g is the LHV for the gaseous fuel, KJ/kg.

$$BTE\ (\%) = \frac{BP}{\boldsymbol{m_{pd}}\ x\ LHV_d + m_g x\ LHV_g}\ x\ 100 \quad \text{(A5)}$$

$$BTE\ (\%) = \frac{BP}{m_d\ x\ LHV_d}\ x\ 100 \quad \text{(A6)}$$

The diesel replacement rate (*Z*) was calculated using Eq. (A7), where *Z* is the mass-based diesel displacement rate, %, m_d is the mass flow rate of diesel used for diesel baseline runs, kg/h, and m_{pd} is the mass flow rate of pilot diesel in dual fuel mode, kg/h.

$$Z\ (\%) = \frac{m_d - m_{pd}}{m_d}\ x\ 100 \quad \text{(A7)}$$

The Φ in dual fuel mode was calculated using Eq. (A8) and for DBL was calculated using Eq. (A9), where Φ_{df} is the equivalence ratio in dual fuel mode and Φ_{DBL} is the equivalence ratio for diesel baseline. The m_{pd} is the mass flow rate of pilot diesel in dual fuel mode, kg/h, m_d is the mass flow rate of diesel used for diesel baseline, kg/h, m_g is the mass flow rate of syngas, kg/h, $AFR_{stoic\text{-}diesel}$ is the stoichiometric air to flow ratio of diesel, and $AFR_{stoic\text{-}gas}$ is the stoichiometric air to flow ratio of gaseous fuel.

$$\phi_{df} = \frac{(m_{pd}\ x\ AFR_{stoich-diesel}) + (m_g\ x AFR_{stoic-gas})}{m_{DF\ air}} \quad \text{(A8)}$$

$$\phi_{DBL} = \frac{m_d\ x\ AFR_{stoich-diesel}}{m_{DBL\ air}} \quad \text{(A9)}$$

This Emission Index (*EI*) value expressed for each pollutant expressed as g/kg fuel was calculated using Eq. (A10). The fixed values for the conversion coefficient used per pollutant are as follows: kCO = 0.971, kCO_2 = 1.526, kTHC = 0.555 (THC measured as methane equivalent), kNO_x = 1.595 (all NO_x is counted as NO_2), N_2O = 1.526 and CO_2 =1.526. In Eq. (A11), k_{gas} = conversion coefficient of the gaseous pollutant, C_i is the concentration of a gaseous pollutant (in ppm or %). If the concentration is measured in ppm, the equation is multiplied by 10^{-6}, if measured in % then the equation is multiplied by 10^{-2}. *AFR* is either AFR_{DBL} or AFR_{df} depending on if this data is calculated for diesel baseline or dual-fuel mode.

$$Gas\ EI = k_{gas} x\ C_i\ x\ (1 + AFR)\ x\ 1{,}000 \quad \text{(A10)}$$

The *EI* (g/kg fuel) was converted further and expressed as *EI* g/MJ fuel using Eq. (A11). Here, *Gas EI* is the emission index value for each pollutant, g/kg fuel, and $LHV_{df\ blend}$ is the LHV of the combined fuel, i.e., the pilot diesel and the syngas, MJ/kg.

$$EI\ (g|MJ\ fuel) = \left(\frac{Gas\ EI}{LHV_{df\ blend}}\right) \quad \text{(A11)}$$

The LHV of the dual fuel blend ($LHV_{df\ blend}$) was calculated in MJ/kg using Eq. (A12). Here, m_{pd} is the mass flow rate of pilot diesel in dual fuel mode, kg/h, m_g is the mass flow rate of syngas, kg/h, LHV_d is the LHV of diesel, MJ/kg, and LHV_g is the LHV for the gaseous fuel, MJ/kg.

$$LHV_{df\ blend} = \left(\frac{m_{pd}}{m_{pd}+ m_g} x\ LHV_d\right) + \left(\frac{m_g}{m_g+m_{pd}} x\ LHV_g\right) \quad \text{(A12)}$$

Gas SE is the Specific Emission data for each pollutant, g/kWh was calculated using Eq. (A13). Here, *Gas EI* is the emission index value for each pollutant, g/MJ fuel and *SEC* is the specific energy consumption for dual fuel mode, MJ/kWh

$$Gas\ SE = Gas\ EI\ (\frac{g}{MJ})\ \text{x}\ SEC \quad \text{(A13)}$$